Journal of Hydrology 511 (2014) 359–373

Contents lists available at ScienceDirect

Journal of Hydrology

journal homepage: www.elsevier.com/locate/jhydrol

The surface energy balance and its drivers in a boreal peatland fen of northwestern Russia

B.R.K. Runkle [a,*], C. Wille [a], M. Gažovič [b], M. Wilmking [b], L. Kutzbach [a]

[a] Institute of Soil Science, Klima Campus, University of Hamburg, Allende-Platz 2, 20146 Hamburg, Germany
[b] Institute of Botany and Landscape Ecology, Ernst Moritz Arndt University Greifswald, Grimmer Straße 88, 17487 Greifswald, Germany

ARTICLE INFO

Article history:
Received 30 August 2013
Received in revised form 23 December 2013
Accepted 25 January 2014
Available online 4 February 2014
This manuscript was handled by Konstantine P. Georgakakos, Editor-in-Chief, with the assistance of Matthew McCabe, Associate Editor

Keywords:
Energy balance
Evaporation
Boreal peatland
Fen
Russia
Eddy covariance

SUMMARY

Boreal peatland energy balances using the eddy covariance technique have previously been made in Alaska, Canada, Scandinavia, and Western Siberia, but not in the European portion of the Russian Federation. European Russia contains approximately 200,000 km^2 of peatlands and has a boreal (subarctic), continental climate influencing the region's energy balance. To help fill this research gap, the surface energy balance was determined for a boreal peatland fen in the Komi Republic of Russia for an 11-month period in 2008–2009 using the eddy covariance method. The total measurement period's cumulative energy balance closure rate was 86%, with higher closure during the critical summer growing season. Similar to other boreal peatland sites, the mid-summer shortwave radiation demonstrated albedo between 0.13 and 0.19 as calculated on a cumulative monthly basis, whereas monthly albedo was >0.9 during the months with greatest snow (January, February 2009). Mid-summer Bowen ratios averaged 0.20–0.25 on a cumulative basis, with monthly averaged mid-day values in the range 0.35–0.53 during the growing season. Latent energy (LE) fluxes exceeded 70% of net radiation and 60% of potential evapotranspiration. During the study period, total evapotranspiration (406 mm) was slightly greater than rainfall (389 mm), with later snowfalls creating excess moisture in the atmospheric water budget. These characteristics together point to a peatland whose energy balance behavior is generally consistent with data from other boreal fens. The LE fluxes were dominantly controlled by net radiation, with less canopy resistance than at other northern fens and a lighter role for vapor pressure deficit to play in the energy balance. The aerodynamic and canopy conductance terms were of similar magnitude, both through the season and through any given diurnal cycle. The consequently high decoupling coefficient (0.65 ± 0.16 in the growing season) allows further modeling of fens in this region with reduced effects from the uncertainties of parameterizing surface conductance terms and their responses to water table and vapor pressure deficit changes. The Priestley–Taylor method provides a reasonable approach to modeling evapotranspiration, given some assumptions about the site's energy balance closure. This understanding of the local drivers on the energy and water budgets has important implications for peatland ecology and growth, regional carbon dynamics, and downstream hydrology.

1. Introduction

Boreal peatlands cover 3% of the earth's land surface and contain 500 ± 100 Pg of organic carbon over their total peat depths (Yu, 2012), which is equivalent to 21% of the 2344 Pg that compose the global organic carbon stock stored in the first three meters of soil (Batjes, 1996; Jobbágy and Jackson, 2000). They are also susceptible to rapid changes in response to increased Arctic-region climate changes and variability (Bridgham et al., 2008; Dise, 2009). Recent studies have focused on the interactions between hydrology and the carbon cycle in these environments, and there is general consensus that the hydrological cycle is an important first-order control to carbon fluxes, vegetation cover and changes, and on micro-topographic patterning (Billett et al., 2004; Couwenberg and Joosten, 2005; Limpens et al., 2008). Peatland hydrology, ecological functioning, and development are largely dependent on the local energy balance and whether precipitation is balanced by evapotranspiration (ET). Additional considerations include the effects of sensible (H) and ground (G) heat flux on the soil or moss surface temperature, which are critical for regulating bacterial activity and CO_2 or CH_4 production (Frolking et al., 2011).

The primary driver of latent energy fluxes (LE) in wetlands is generally seen to be net radiation (R_n), with wetland LE/R_n ratios

* Corresponding author. Tel.: +49 40 42838 2010; fax: +49 40 42838 2024.
E-mail address: benjamin.runkle@zmaw.de (B.R.K. Runkle).

http://dx.doi.org/10.1016/j.jhydrol.2014.01.056
0022-1694/

generally exceeding 0.5 and fen values generally higher than bog values (Lafleur, 2008). The effect of the water table position is often of lesser importance though it does help determine canopy conductance (g_c) as it controls the relative contributions of different ground components such as bare soil, mosses, or vascular plants (Lafleur et al., 2005; Sonnentag et al., 2010). Other studies have found some positive effect from lower water tables on ET, but these impacts may be confounded by the coupling to the synoptic meteorological conditions driving the water table conditions (i.e., less precipitation and higher vapor pressure deficit – VPD) (Wu et al., 2010). Tests of the peatland energy balance in land surface modeling schemes have estimated more accurate fluxes for fens than for bogs, in part due to the complexities of moss evaporation and its link to water table height, which often varies irregularly through a site (Comer et al., 2000).

The European part of Russia includes approximately 200,000 km^2 of peatlands, mostly in its boreal regions, thus composing more than 50% of the world's boreal peatland landscapes (Apps et al., 1993; Joosten et al., 2012). The potential of these sites for long-term carbon uptake is not assured due to a variety of climatic and biological factors ranging from increased temperature to carbon saturation in the sink mechanisms. While most research on northern peatlands focuses on Alaska, Canada, and Scandinavia, some energy flux research has been performed in the Russian taiga wetlands (Kurbatova et al., 2002). Their water relations and energy balances have long been studied (Romanov, 1968a; Ivanov, 1981), but the results of this research are often under-reported or delayed in English-language literature (Masing et al., 2010). For example, one relatively recent report (Shutov, 2004) describes the water balances of boreal peatland bogs in northwest European Russia based on investigations with weighing lysimeters in the 1970s. This report found significant reductions in peatland evaporation as the summer water level dropped below the threshold where the surface peat was wetted by the capillary fringe (i.e., to −50 cm). Comparing results from relatively wet and dry years, the authors found similar rates of evapotranspiration and assume it is driven more by vegetation cover than by water availability. As a result, in the relatively wet year, the ratio between evapotranspiration (ET) and precipitation (P), used as a climate wetness index with implications for peat growth and hydrology, was 0.38 whereas in the dry year the ET/P ratio was 0.47. In both cases, ET was 63% of global solar radiation so the change in the ET/P ratio was derived nearly entirely by the reduction in P rather than a change in ET. In contrast to the relative consistency of ET rates in different climate conditions, the authors do find spatial heterogeneity of ET across their peatland landscape, with open water and lake-filled regions evaporating more water than a hollow-ridge complex consisting of some bare peat surfaces.

There is some history of work using the eddy covariance methodology (Baldocchi, 2003) to determine the energy balance and drivers of evapotranspiration in the continental peatlands of Russia. For instance, a comparison between a European bog (Fyodorovskoye) and a central Siberian bog (Zotino) revealed strong LE fluxes relative to H, with higher Bowen ratios (H/LE) in Fyodorovskoye (the approximate mid-summer average of a 5-day running mean ratio was 0.6–0.8 vs. 0.3, respectively) (Kurbatova et al., 2002). Both sites were characterized by close surface–atmospheric coupling through the effect of surface drying, limiting the role of net radiation in driving evaporative fluxes. This finding is in contrast to other work in a western Siberia bog (Shimoyama et al., 2004) that found a strong decoupling and therefore a large role for net radiation in driving the latent energy flux. Despite these studies, however, examples of the energy balance in Russian peatlands remain rare with a relative paucity of data compared to other regions (Lafleur, 2008; Wang and Dickinson, 2012). Finally, Russia's peatlands contain a diversity of hydro-ecological forms (Minayeva and Sirin, 2012), and there seem to be no reports of Russian boreal fen energy balances in the eddy covariance literature.

Therefore the key objective of this study is to quantify and describe the diurnal and seasonal variations and drivers of the energy balance for a typical boreal peatland complex of the Russian Federation's Komi Republic. This site, like many in this region, contains both fen-like and bog-like portions. However, since the predominant wind direction at our measurement site created an average measurement footprint covering the fen portion, that region was made the focus of the study. This work compares the relative contributions of net radiation and vapor pressure deficit to controlling latent energy fluxes. It also explores drivers of canopy conductance and how these factors change over time. Finally, an 11-month energy balance is generated, and the evapotranspiration fluxes are contextualized within the water balance, including measured changes in the water table and rates of precipitation and snowfall.

2. Methods and site description

2.1. Site description and data collection

The study site is a typical river valley peatland in North-West Russia called the Ust-Pojeg mire complex (61°56′N, 50°13′E, 119 m a.s.l.) in the middle taiga region (Lopatin et al., 2008) of the Komi Republic (Fig. 1). The Komi Republic is at the eastern edge of European Russia and has a humid continental climate with warm summers and consistently freezing winter temperatures with continuous snow cover. The mean annual rainfall of Syktyvkar, capital of the Komi Republic and 50 km southeast of the field site, is 525 mm (1888–2012), and the mean annual temperature is 1.1 °C (RIHMI-WDC, 2013).

The river valley peatland site is in a transitional state from fen to bog following paludification and so consists of minerogenous, ombrogenous, and transitional zones; it lies within a region of the Komi Republic that has been classified as mainly containing ombrotrophic raised bogs (Vasander, 2007) and is not underlain by permafrost. The vegetation is dominated by sedges, dwarf shrubs, and *Sphagnum* mosses, and small microtopographic features such as hummocks, hollows, and lawns are evident. A transect survey through the site revealed peat depths of up to 2 m, and radiocarbon dating of the basal peat suggests that the peat development was initiated between 7500 and 9500 years ago, or even earlier (Pluchon, 2009).

The site's vegetation characteristics change in accord with the transitions between ombrogenous and minerogenous areas (Schneider et al., 2012). The ombrogenous bog in the site's northern part is dominated by *Sphagnum angustifolium* with dwarf *Pinus sylvestris* trees on hummocks. The minerogenous fen region in the south part contains *Sphagnum jensenii* and *Utricularia intermedia*. The transition region between the fen and bog parts of the peatland contains *Carex rostrata* lawns. Throughout the peatland the microrelief is further distinguished as tending to be composed of drier, elevated hummocks covered by *Andromeda polifolia*, *Chamaedaphne calyculata*, *Betula nana* and *P. sylvestris*; wetter hollows are composed primarily of *Scheuchzeria palustris* and *Carex limosa*. Canopy height and leaf area index therefore varied considerably through the site, though a reasonable average canopy height is approximately 20 cm. The vascular plant green leaf area index (GAI) was determined through measurements of leaf size and number in biweekly assays in 18 plots (60 cm × 60 cm; only the 9 plots in minerogenic areas are used for the GAI estimates referenced here); living moss cover was estimated as 0.75 $m^2\ m^{-2}$ through the growing season (Schneider et al., 2012).

An eddy covariance system with a closed-path CO_2 and H_2O gas analyzer (Li-7000, Li-COR Biosciences, USA) was used to measure

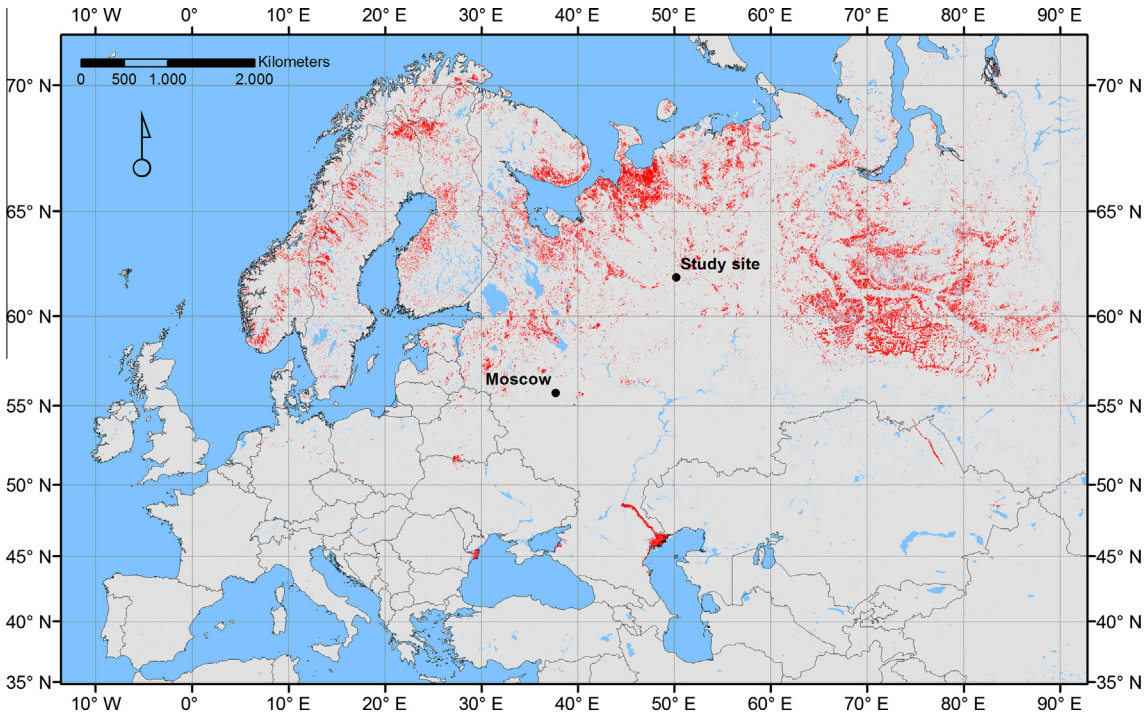

Fig. 1. Map showing Ust-Pojeg field site location within Europe. Points marked in red indicate wetland land cover types determined in the ESA GlobCover 2009 product at a 300 m resolution using the MERIS sensor (ESA, 2010).

the turbulent fluxes of momentum, heat, CO_2 and H_2O from 1 April 2008 until 12 February 2009 (Gažovič et al., 2010). An ultrasonic anemometer (R3-100, Gill Instruments, UK) measured wind velocity components in three dimensions and sonic temperature at 20 Hz frequency at a height of 3 m. Sample air was drawn at a rate of 8.5 L min^{-1} from the air intake close to the anemometer measurement point, through a high-density polyethylene tube of 12 m length and 4 mm inner diameter, and through the closed-path gas analyzer. At the time of the start of measurements, the tube was new, i.e. the inner tube walls were uncontaminated. The site's fetch is relatively flat and homogeneous despite the microtopographic variation in the peatland surface. Initial investigation of the CO_2 data collected in this campaign indicates a growing season length of approximately 120 days, from DOY 140 to 260, or 19 May to 16 Sept, based on positive 24-h net ecosystem productivity (Gažovič et al., in preparation).

This site was supported by an adjacent meteorological station that collected data on relative humidity (RH) and air temperature (T_a) (CS215, Campbell Scientific Ltd., UK), air pressure (RPT410F, Druck Inc., USA) and four-component radiation (CNR 1, Kipp and Zonen, Netherlands). Surface temperature (T_s) was determined from the outgoing long-wave radiation measurement with the Stefan–Boltzmann law and an assumed emissivity of 0.98; it is used to decide when to apply the latent heat of sublimation (at $T_s < 0$ °C) in place of latent heat of evaporation in converting water vapor fluxes to latent energy fluxes. Soil temperature at 1 cm and 5 cm below the peat surface was measured by CS-107 temperature probes (Campbell Scientific Ltd., UK) and heat flux plates (HFP01, Hukseflux, NL) measured at two nearby positions at a depth of 5 cm. Rainfall was measured by a HOBO RG2 tipping bucket rain gauge (Onset Computer Corporation Inc., USA), water level in the fen was measured by MDS Dipper groundwater loggers (SEBA Hydrometrie GmbH, Germany), and photosynthetically active radiation (PAR) was measured by an SKP215 sensor (Skye Instruments Ltd., UK). Vapor pressure deficit (*VPD*) was determined from *RH* and T_a using a vapor pressure saturation curve (Bolton, 1980). Water level fluctuations are compared to precipitation and evapotranspiration in the vertical (land–atmosphere) water balance by assuming a specific yield (S_y) of 0.60, which has been estimated for the upper layers of other boreal peatlands (Petrone et al., 2008). Snow cover and water content was determined through a series of seven vertical profile measurements in a transect line through the peatland over eight days between 27 March and 10 April 2008 and again during the period between 3 February and 10 February 2009. These data were supplemented by snow and precipitation data from the meteorological station at Syktyvkar, approximately 50 km to the southeast. All data are reported in local time, which is UTC + 4 h.

2.2. Eddy covariance data processing

Our flux data processing and correction routine is similar to one used in previous studies at this site (Runkle et al., 2012), and includes data screens based on stationarity and integral turbulence characteristics (Foken and Wichura, 1996). The processing routine uses a peak-detection algorithm in order to more accurately capture the delayed lag time possible under higher humidity and low-flux conditions and applies it in the flux data-processing routine after coordinate rotation of the wind velocity vectors. Corrections for tube attenuation of water vapor, based on cospectral similarity to the heat flux signal, are applied on the data until 15 October 2008 because a inlet tube heating cable installed at that time changed and largely eliminated this response (Runkle et al., 2012). Calculations have been performed using EdiRe v1.5 (R. Clement, University of Edinburgh, UK) for flux data processing and Matlab v7.13 2011b (Mathworks, Inc., USA) for other numerical analyses.

Gap-filling on the time series of the turbulent energy fluxes (H and LE) was performed using an automated moving window, semi-empirical look-up method based on the response of these fluxes with VPD, T_a, and incoming solar radiation (R_s) (Falge et al., 2001; Reichstein et al., 2005). Once screened for wind direction

to remove the non-fen-like segments, gap-filling was required for 50% of LE measurement intervals and 40% of H measurement intervals. For certain months, the gap-filling requirements were higher; i.e., October's dataset required 78% of the half-hour periods to be filled, January required 71% and February required 91%. The other measured months required 38–53% of time periods to be gap-filled. The LE flux was further gap-filled using several modeling techniques described below. Footprint modeling was performed using an analytical model that assumes height-independent crosswind dispersion and that the vertical turbulent mixing process is stationary and behaves as a gradient analogous to diffusion (Kormann and Meixner, 2001). This approach has been applied to other boreal peatland sites (Forbrich et al., 2011) and is used primarily to distinguish between the fen-like and bog-like portions of the site.

2.3. Energy balance and modeling evapotranspiration

The surface energy balance is composed of net radiation (R_n), ground heat flux (G), the turbulent sensible heat flux (H), the turbulent latent heat flux (LE), the energy used to melt snow (Q_m), and a closure term or residual to account for an incomplete balance through measurement error or missing terms (C):

$$R_n = G + \mathrm{LE} + H + Q_m + C \tag{1}$$

The sign convention used is that R_n and G are positive downward and H and LE are positive upward. Q_m is positive when the snow melts.

Q_m is modeled using the specific latent heat of fusion of water (L_f, 0.33 MJ kg^{-1}). For the April 2008 period, the snowpack's water equivalent (SWE) was measured on site and used with L_f. For the following winter SWE was derived from the Syktyvkar weather station's precipitation data. A degree-day snowmelt model was then applied using a 0 °C reference temperature and an open-area melt-rate factor of 4 mm °C^{-1} d^{-1} (Rango and Martinec, 1995). This modeled melt water amount is then converted to the energy term Q_m using L_f. A sensitivity analysis of this factor conducted by shifting it between 3 and 5 mm °C^{-1} d^{-1} revealed only slight impact (3–5 days) on the timing of snowmelt and a statistically indistinguishable effect on the 30-min energy balance closure. As a diagnostic indicator of the performance of the eddy covariance technique, the energy balance closure is evaluated by using the half-hourly measurements and finding the least-squares linear regression slope EB–C_{30} and intercept EB–C_{30i}, of the equation (LE + H) = EB–C_{30} * ($R_n - G - Q_m$) + EB – C_{30i} (as presented in Wilson and Baldocchi, 2000).

LE (i.e., ET Leρw) is modeled and gap-filled using the Penman–Monteith equation:

$$\mathrm{ET} = \frac{1}{L_e \rho_w} \cdot \frac{sR_a + c_p \rho_a VPD g_a}{s + \gamma(1 + g_a/g_c)} \tag{2}$$

where R_a is the available energy and is approximated from the sum of H and LE. Alternatively and perhaps more traditionally, $R_n - G - Q_m$ is used, but the potential mismatch in their footprints and the difficulty of a good spatial estimate of G across the site's microtopography preclude this option here. The other terms are aerodynamic conductance (g_a), surface or canopy conductance (g_c), the slope of the saturation vapor pressure curve against temperature (s), the psychrometric constant (γ), the density of water (ρ_w) and dry air (ρ_a), the latent energy of evaporation (L_e), the heat capacity of air (c_p), and the vapor pressure deficit (VPD). This model can be modified to estimate the potential evapotranspiration rate (PET) by setting g_c to infinity. The model is inverted to create estimates of g_c based on measured LE.

When the sonic anemometer provided quality-controlled estimates of u_*, a formula for g_a is computed to include excess boundary resistance to heat and water vapor transport. This approach has been used in previous studies of peatland landscapes (Kim and Verma, 1996; Humphreys et al., 2006), referencing work describing flow over irregular surface elements (Wesely and Hicks, 1977; Verma, 1989):

$$g_a = \left(\frac{kB^{-1}}{k u_*} \left(\frac{d_h}{d_v} \right)^{2/3} + \frac{u}{u_*^2} \right)^{-1} \tag{3}$$

where u_* is the friction velocity, u is the mean wind speed, k is the von Karman constant with a value of 0.4, and d_h/d_v is the ratio of thermal diffusivity (d_h) to molecular diffusivity of water vapor (d_v) and is set to 0.89 at 20 °C. The kB^{-1} term, using the dimensionless parameter B^{-1}, is an estimate of the logarithmic ratio between the roughness length of momentum and the roughness length for mass or sensible heat fluxes (Owen and Thomson, 1963). A kB^{-1} value of 2 is used for comparison to a recent review of the peatland energy balance (Humphreys et al., 2006), though slightly lower (1.6) and higher (2.3) values have also been used in peatland studies (Campbell and Williamson, 1997; Shimoyama et al., 2004). The two conductance terms are determined on a half-hourly basis but are presented using monthly and diurnal average values; they are also determined separately for wet or dry periods as defined as the presence (or absence) of rainfall in the preceding 12 h (Brümmer et al., 2012).

The surface roughness length z_0 is determined from the sonic anemometer's 30-min estimate of u_* and mean wind speed, similar to Sonnentag et al. (2011):

$$z_0 = \frac{z - d_0}{\exp(k * u/u_*)} \tag{6}$$

where z is the measurement height (3 m), d_0 is the zero-displacement height (assumed to be 0.66 * h) and z_0 is assumed to be 0.1 * h (Foken, 2008), where h is the vegetation canopy height. Therefore, z_0 and h can then be derived from the other terms. This z_0 parameter is derived under near-neutral conditions ($|z/L| < 0.025$) and high mean horizontal wind speeds ($u > 3$ m s^{-1}) to ensure minimal correlation between z_0 and u. A seasonal evolution of z_0 is then developed based on the monthly mean z_0 estimates, interpolated through time, and used to generate estimates of u_* from the meteorological wind sensor when the sonic anemometer's performance failed quality control.

Measured and modeled evapotranspiration can also be compared to equilibrium evaporation E_{eq} (McNaughton, 1976). This rate represents the vapor flux expected from an extensive moist surface in the absence of advective influences (as it is missing the u, VPD, and conductance terms of the Penman–Monteith equation):

$$\mathrm{ET_{eq}} = \frac{1}{L_e \rho_w} \cdot \frac{sR_a}{s + \gamma} \tag{7}$$

where R_a is the available energy, which is defined either as ($R_n - G - Q_m$) or as (H + LE). Both terms are used in the literature and offer a chance to explore the effect of the incomplete energy balance closure on the Priestley–Taylor (1972) relationship, which uses $\mathrm{ET_{eq}}$ in the formula ET = α_{PT} $\mathrm{ET_{eq}}$, where α_{PT} is fit through linear regression against measured ET. Some researchers consider the Priestley–Taylor α_{PT} of 1.26 as a truer representation of equilibrium conditions (Eichinger et al., 1996). In either case, α_{PT} can be a useful indicator of the drivers of evaporation, as the fitted value can vary substantially among different wetlands (Roulet and Woo, 1986; Souch et al., 1996).

2.4. Canopy conductance modeling

The canopy conductance is modeled by the following relationship, which modifies relationships used in other wetland studies (Kellner, 2001; Wu et al., 2010) and is fit for the inverted g_c estimates on a monthly basis by minimizing the root-mean-square error of modeled output:

$$g_c = \frac{a \times R_s + b}{1 + c \times \mathrm{VPD}} \quad (8)$$

where R_s is the incoming shortwave radiation and a (mm s^{-1} W^{-1} m^2), b (mm s^{-1}), and c (kPa^{-1}) are the best-fit parameters. This modeled value is used with the Penman–Monteith equation (where $R_a = R_n - G - Q_m$) to gap-fill the full time series of LE fluxes. At a daily time scale, the daytime mean g_c is compared to daytime mean VPD through a relationship used in other peatland energy balance studies (Humphreys et al., 2006; Sottocornola and Kiely, 2010):

$$g_c = \frac{g_{c,\max}}{1 + b_D \times \mathrm{VPD}} \quad (9)$$

In this relationship, $g_{c,\max}$ (mm s^{-1}) and b_D (kPa^{-1}) are best-fit parameters similar to b and c in the previous equation. This relationship is fit for daytime intervals with PAR >400 μmol m^{-2} s^{-1}, which is a lower light threshold than used in comparative studies, but allows more data from a wider portion of the growing season to be examined.

The decoupling coefficient can also be used to quantify the degree of interaction between the evaporating surface and the atmosphere outside of the leaf boundary layer (McNaughton and Jarvis, 1983; Jarvis and McNaughton, 1986):

$$\Omega = \frac{s/\gamma + 1}{s/\gamma + 1 + g_a/g_c} \quad (10)$$

An Ω value near 0 implies a strong coupling between atmosphere and vegetation so that VPD in the region of the leaf (or otherwise evaporating surface) is negligibly distinct from VPD in the atmosphere. In these cases, $g_c \ll g_a$ and E is primarily controlled by g_c and VPD. Alternatively, a Ω of 1 implies complete decoupling of LE and the atmospheric moisture budget, as R_n is the only contributor to E ($g_c \gg g_a$) and changes in evaporation tend to have no effect on VPD in the region of the evaporating surface. Such decoupled conditions may develop in the moist microclimates within a forest canopy or a wet landscape, while coupling tends to be stronger in drier, more water-limited ecosystems, including peatlands if the moss surface dries out.

2.5. Ground heat flux

The ground heat flux plate measurements (G_5) at 5 cm depth (Δz) were corrected for changes in heat storage in the overlying peat layers using the combination method of C.B. Tanner (Brutsaert, 1982; Drexler et al., 2004). This method uses the difference of the average peat temperature measured at both 1 cm and 5 cm over a 30-min interval (dT_{1-5}), assumes a constant heat capacity (C_h) in time (t) and space (z), and uses dt set to 1800 s (the measurement interval of the ground heat flux plate):

$$G = G_5 + C_h \frac{dT_{1-5}}{dt} \Delta z \quad (11)$$

A weighted heat capacity was used by assuming continuously saturated peat conditions and porosity 0.8. This value (3.54 MJ m^{-3} K^{-1}) assumes constant heat capacities of dry peat soil (2.3 MJ m^{-3} K^{-1}) and of water (4.2 MJ m^{-3} K^{-1}). The mean corrected ground heat flux from each plate measurement for each 30-min interval was used to average the effects of spatial heterogeneity in heat conduction.

3. Results

3.1. Site energy balance

The site's observed meteorological conditions reflected its position in the boreal zone, with cold, extended freezing conditions in winter and warm summer months in June and July (Fig. 2). At the Syktyvkar meteorological station, the study year of 2008 was both warmer and wetter than long term annual average conditions with a mean annual temperature of 3.4 °C and a precipitation of 687 mm (water equivalent) from April 2008 to February 2009 (though the installed station at the study site measured only 486 mm precipitation). Relative to long-term conditions, the study year had higher than average temperatures in July and the winter months and more rainfall in August largely due to a single storm event.

Near the start of field measurements, on 6 April 2008, the peatland surface was completely covered with a snow layer of approximately 40 cm depth (with average volumetric water content of 29%, representing 36 MJ m^{-2} cumulative melt energy or one-third of April's net radiation). This time was followed soon after by rain events and higher temperatures, melting all snow and contributing to a rise in the water table. From 16 April, the water table was near the surface on hummock locations and from +5 to +17 cm over the peat surface in transitional to minerogenic regions, respectively. These water surfaces dropped by 3–9 cm from 21 April to 3 May, during a period with pronounced daily temperature fluctuation and nighttime freezing of the water and peat surfaces (Gažovič et al., 2010). Despite punctuation by small precipitation events, the water table continued on a general decline to −14 cm until a large (36 mm) rain event 19–20 August and subsequent rainfall brought the mean water table up toward the surface. Examining solar albedo from the 4-component radiometer suggests a first winter snowfall on 5 November 2008, followed by a brief melt event one week later, and then near continuous site snow cover until the end of the measurement campaign.

The eddy covariance measurements were screened for quality and footprint to generate time series for LE and H. As a diagnostic of the half-hourly flux measurements, the site achieved a 75% closure slope (i.e., EB–C_{30} at of the full dataset), though closure was much higher in the summer months (EB–C_{30} of 0.73 in September to EB–C_{30} of 0.97 in July and August). Moreover, the gap-filled cumulative annual energy balance was 86% of incoming radiation (Tables 1 and 2). The dominant wind direction generated a seasonal eddy flux footprint weighted toward the site's fen-like portions, with much less data representing the mire's bog regions. Of the 30-min eddy flux intervals that passed data-screening and technical concerns, 78% were from wind directions (124–327°) where 50% or more of the flux-contributing areas were within the fen region. No consistent changes to the energy partition were found to differentiate the bog and fen contributing regions during meteorologically similar data collection intervals. The result of these screens was that 50% of the measurement period's half-hourly data was kept for further analysis. The footprint model additionally demonstrated that in 96% of the flux measurement periods, 80% of the flux footprint was within 500 m of the eddy tower, thus largely avoiding the patches of forest on the mire's outskirts. The remainder of flux measurements occurred during stable, night-time conditions with low fluxes and so had little effect on the total energy balance, and the region of maximum contribution to the overall flux at these times was still well within the open peatland's boundaries. The lookup-table method was successful in generating gap-filled H fluxes with root-mean-square error (rmse) of 13.6 W m^{-2}, determined by comparing measured data to the modeled values estimated from

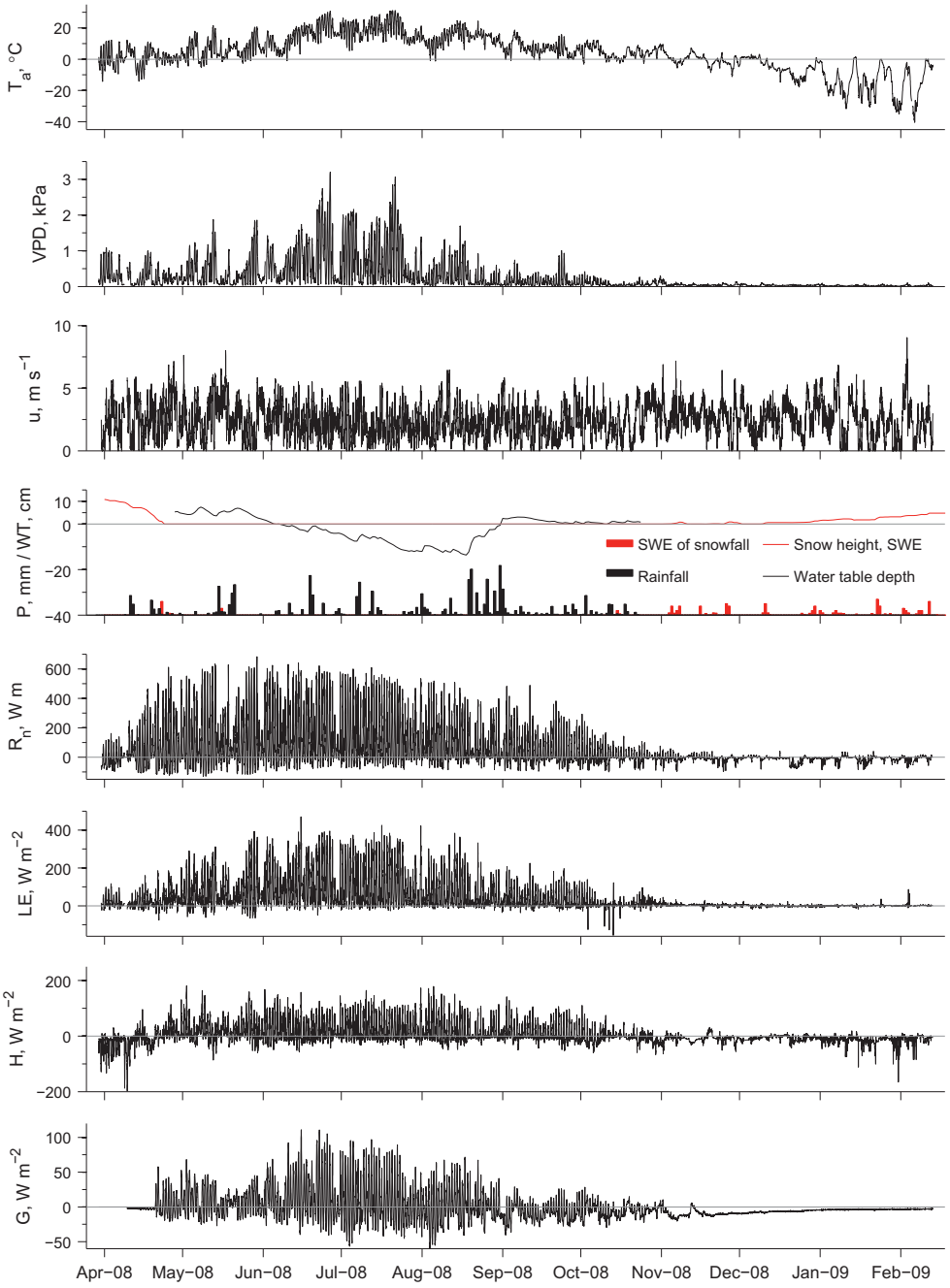

Fig. 2. Meteorological conditions and gap-filled energy fluxes derived from the eddy-covariance methodology (or ground heat flux modeling) for 2008–2009 field year, measured or modeled on a half-hourly frequency. Measured meteorological terms include air temperature (T_a), vapor pressure deficit (VPD), horizontal wind speed (u), and precipitation (P), which represents rainfall (in black) and the water-equivalent of snow (in red). The water table depth (WT) is the mean of two wells in the fen region of the peatland site. Note the changing y-axis limits on the heat fluxes—net radiation (R_n), latent energy (LE), sensible heat (H), and ground heat flux (G). (For interpretation of the references to color in this figure legend, the reader is referred to the web version of this article.)

the gap-filling technique. Compared to the measured data points, modeled LE fluxes had rmse of 23.0 W m^{-2} using the lookup-table method and improved to rmse of 12.2 W m^{-2} using the Penman–Monteith model with parameters presented below.

The magnitude of the energy fluxes closely followed net radiation (Tables 1 and 2), which during the unfrozen months was largely partitioned into latent energy flux (>60%). Because of substantial winter-time negative sensible heat fluxes, LE represented 77% of the measurement period energy balance. During the growing season, H reached nearly 20% of the monthly energy balance and G approached 10% (in June). Compared to potential evapotranspiration, total actual evapotranspiration during the summer was in the range 61–67% and often exceeded total equilibrium evapotranspiration. The monthly averaged growing season shortwave albedo was between 10% and 19%, and the summer R_n/SW$_{in}$ ratio was in the range 0.56–0.61. The cumulative monthly Bowen ratio (i.e., H/LE including both night and day values) had high values of 0.28 in September and May but was as low as 0.20 in June and was 0.08 for the complete 11-month measurement period (lowered by strongly negative sensible heat fluxes during

Table 1
Monthly cumulative surface energy balance terms[a] with units MJ m^{-2}.

Month	R_n	H	LE	G	Q_m	C	LE_{pot}	LE_{eq}	LW_{in}	LW_{out}	SW_{in}	SW_{out}
April 2008	108	−27	63	1	39	31	125	37	669	803	380	134
May 2008	278	51	183	20	1	23	272	143	766	936	497	50
June 2008	355	49	252	36	0	17	378	210	860	1004	580	78
July 2008	360	64	260	19	0	18	424	242	942	1091	620	111
August 2008	193	34	140	0	0	19	212	121	938	1023	343	66
September 2008	98	21	75	−21	0	24	122	64	816	900	216	34
October 2008	12	−19	23	−15	1	22	50	12	840	889	73	12
November 2008	−20	−24	11	−25	7	11	26	−1	775	805	19	9
December 2008	−32	−20	3	−18	3	1	15	−3	741	774	11	9
January 2009	−33	−42	2	−10	1	16	5	−5	613	647	33	32
Feb.09[b]	−9	−11	2	−3	0	3	3	−1	250	261	22	20
Total	1310	77	1014	−16	52	183	1630	819	8211	9134	2794	554

[a] Sensible heat flux (H) is derived from a look-up approach gap-filling tool on eddy covariance data. Latent energy (LE) is gap-filled with the Penman–Monteith model described in the text. Net radiation (R_n) and incoming and outgoing short- and long-wave radiation (SW_{in}, SW_{out}, LW_{in}, LW_{out}) are measured using a net radiometer and 4-component radiometer, respectively. Ground heat flux (G) is measured with heat flux plates and corrected for changes in heat storage in the overlying peat layers, the energy required for snow melt (Q_m) is modeled based on measured snow height and density, and C indicates the residual. Potential (LE_{pot}) and equivalent (LE_{eq}) latent energy fluxes are modeled as described in the text.

[b] The measurement campaign concluded 12 February 2009, so February is presented as a partial month.

Table 2
Monthly ratios of key energy balance terms, where "Annual" implies ratios derived from the study period's total radiation components. $B_{r,mid\text{-}day}$ refers to the average half-hourly Bowen ratio (H/LE) for the mid-day period (10:00–14:00 h), and the standard deviation is given as the uncertainty range; the "Annual" value given for this term only refers to the growing season, defined as between 19 May and 16 September. EB−C_{30} and EB−C_{30i} refer to the diagnostic energy balance closure slope and intercept, respectively, from the 30-min measurement intervals. Other abbreviations are the same as in Table 1 and the text.

Month	LE/R_n	H/LE	H/R_n	G/R_n	C/R_n	LE/LE_{pot}	R_n/SW_{in}	SW_{out}/SW_{in}	$B_{r,mid\text{-}day}$	EB−C_{30}	EB−C_{30i}, W m^{-2}
April 2008	0.59	−0.43	−0.25	0.01	0.29	0.50	0.28	0.35	0.01 ± 2.48	29.2 ± 1.4	0.23 ± 0.06
May 2008	0.66	0.28	0.18	0.07	0.08	0.67	0.56	0.10	0.53 ± 0.33	61.5 ± 0.9	0.50 ± 0.03
June 2008	0.71	0.20	0.14	0.10	0.05	0.67	0.61	0.13	0.35 ± 0.20	82.6 ± 0.8	0.77 ± 0.04
July 2008	0.72	0.25	0.18	0.05	0.05	0.61	0.58	0.18	0.37 ± 0.19	96.5 ± 0.7	0.97 ± 0.04
August 2008	0.72	0.25	0.18	0.00	0.10	0.66	0.56	0.19	0.47 ± 0.18	96.9 ± 0.9	0.97 ± 0.04
September 2008	0.76	0.28	0.21	−0.21	0.24	0.61	0.45	0.16	0.68 ± 0.24	72.9 ± 0.8	0.70 ± 0.04
October 2008	1.95	−0.83	−1.61	−1.22	1.81	0.47	0.16	0.16	0.27 ± 1.39	64.9 ± 2.2	0.69 ± 0.08
November 2008	−0.57	−2.09	1.19	1.28	−0.54	0.43	−1.04	0.47	−0.47 ± 2.82	41.9 ± 2.3	0.41 ± 0.10
December 2008	−0.09	−6.98	0.64	0.56	−0.03	0.20	−2.98	0.87	1.84 ± 6.15	41.9 ± 1.8	0.38 ± 0.07
January 2009	−0.05	−27.06	1.28	0.31	−0.49	0.33	−0.98	0.95	9.11 ± 12.76	49.5 ± 2.1	0.33 ± 0.10
February 2009	−0.22	−5.47	1.18	0.36	−0.31	0.67	−0.41	0.91	21.63 ± 58.98	39.4 ± 5.8	0.39 ± 0.23
Annual	0.77	0.08	0.06	−0.01	0.14	0.62	0.47	0.20	0.47 ± 0.25	75.2 ± 0.4	0.72 ± 0.02

the snow-covered months). Monthly average mid-day Bowen ratios were in the range 0.35–0.68 during the growing season months.

The monthly mean diurnal cycle of the primary energy flux terms revealed the dominance of the latent energy flux within the partition of net radiation at nearly all points of the diurnal cycle for the months with significant incoming net radiation (Fig. 3). While LE generally rose in concert with morning increases in net radiation, it declined more slowly in the late afternoon, as T_a and VPD remained high during this period. During the afternoon and into the evening, LE often met or exceeded R_n. The ratio H/R_n was more constant during daytime hours relative to LE/R_n. This pattern is made explicit through plotting the Bowen ratio's average diurnal cycle in Fig. 5, which demonstrates that early-morning peaks in the H/LE ratio approached 0.85 in some months and then declined during the day. Modeled G peaked approximately 1 h later in the day than R_n and took a higher proportion of R_n earlier in the year than later. During wintertime, latent energy was negligible, and the ground and sensible heat fluxes, which were generally negative, left larger relative energy imbalances in the budget.

The relative strength of R_n and VPD in driving latent energy fluxes changed through the months (see Supplemental Data table). From April through November R_n, was a stronger influence than VPD, with greater coefficient of determination (r^2) on a regression of half-hourly data (up to 0.88 in July; $p < 0.001$). During the months June–August, a regression line determining this control has a slope of 0.56 or greater, though at other times the slope is lower (0.23 ± 0.02 in April, 0.42 ± 0.04 in October, and insignificant during the winter months). The maximum explanatory power of VPD alone on LE was in August ($r^2 = 0.62$, $p < 0.001$) with September sharing a similarly high slope in a regression line between VPD and LE (i.e., 210 W m^{-2} kPa^{-1}). The strong temporal correlation between R_n and VPD (Pearson correlation coefficient $r = 0.64$, $p < 0.001$, across the whole measurement period) precludes determining from these regressions alone whether either's relationship with LE was solely causal.

The parameters and indicators describing different portions of the controls on LE changed over the season and generally tracked vegetation growth as expressed by vascular plant GAI (Table 3). The estimated roughness length z_0 reached a maximum 46 ± 12 mm in August and was 3 ± 2 mm in February. The decoupling coefficient, Ω, had a daytime average value of 0.65 ± 0.16 during the full measurement period but was slightly higher during the growing season, with a monthly average range of 0.65–0.73 and a standard deviation of approximately 0.14 in each month. This higher decoupling indicates more direct influence of R_n on LE fluxes. The imperfect energy closure has considerable influence on the α_{PT} parameter. During June–August, α_{PT} was in the range 0.97–1.06 when assuming available radiation is equivalent to $R_n - G - Q_m$, whereas these values climbed to 1.06–1.17 when using gap-filled $H + LE$. During these summer months, the Priestley–Taylor relationship is an effective model of LE, with r^2 values between 0.78 and 0.87 (using $R_n - G$), though monthly rmse can exceed 50 W m^{-2}. As a descriptive model using $H + LE$ for

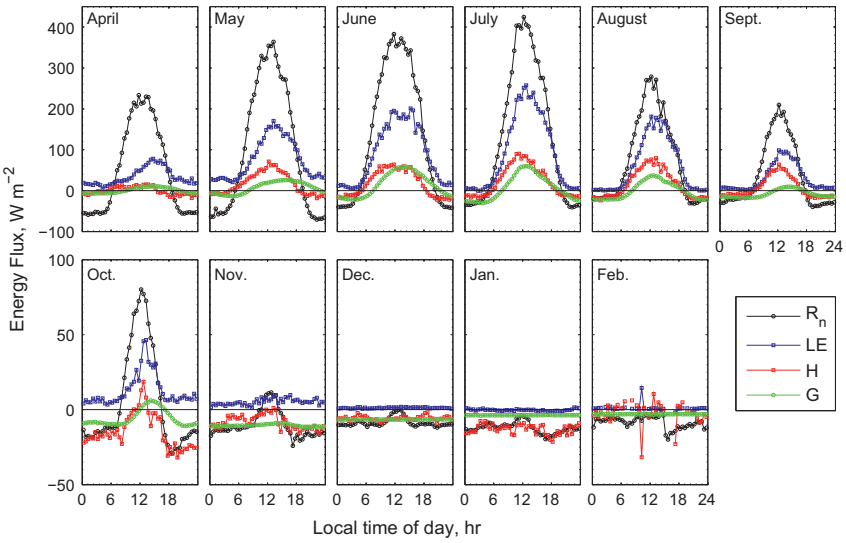

Fig. 3. Monthly mean diurnal pattern of the study site's energy fluxes—net incoming radiation (R_n), latent energy (LE), sensible heat (H), and ground heat flux (G)—during the study period (April 2008–February 2009). The energy required for snowmelt is not shown, but follows the diurnal course of air temperature. Note the change in y-axis scaling between the two rows of plots.

Table 3
Monthly parameters governing and describing conductance and LE fluxes. Vascular plant green area index (GAI) is determined via leaf size and number estimates (Schneider et al., 2012); the roughness length (z_0); decoupling coefficient (Ω), determined when PAR > 20 μmol m^{-2} s^{-1}; and the Priestley–Taylor coefficient (α_{PT}) and its fit statistics are presented. The α_{PT} coefficient and other Priestley–Taylor model terms are determined twice, with different assumptions for the available radiation (R_a), but in both cases use only daytime intervals with PAR > 20 μmol m^{-2} s^{-1}. This model's root-mean-square error (rmse) from measured latent energy flux is used as a fit-statistic and has units of W m^{-2}. Annual values are derived from the full measurement dataset.

Month	GAI	z_0 (mm)	Ω (day)	$R_a = R_n - G - Q_m$			$R_a = H + LE$		
				α_{PT} (day)	r^2, p-Value	rmse	α_{PT} (day)	r^2, p-Value	rmse
April 2008	0	18 ± 10	0.53 ± 0.17	0.54 ± 0.05	0.26, $p < 0.001$	36.24	1.45 ± 0.05	0.76, $p < 0.001$	25.02
May 2008	0.08	26 ± 10	0.67 ± 0.12	0.82 ± 0.03	0.69, $p < 0.001$	52.85	1.34 ± 0.03	0.95, $p < 0.001$	18.8
June 2008	0.43	32 ± 13	0.70 ± 0.13	0.97 ± 0.03	0.78, $p < 0.001$	48.24	1.17 ± 0.03	0.96, $p < 0.001$	21.37
July 2008	1.54	45 ± 12	0.65 ± 0.12	1.02 ± 0.02	0.87, $p < 0.001$	38.86	1.06 ± 0.02	0.98, $p < 0.001$	15.92
August 2008	1.41	46 ± 12	0.67 ± 0.14	1.06 ± 0.03	0.82, $p < 0.001$	36.73	1.08 ± 0.03	0.98, $p < 0.001$	14.33
September 2008	0.33	38 ± 12	0.73 ± 0.14	0.84 ± 0.03	0.58, $p < 0.001$	29.32	1.16 ± 0.03	0.91, $p < 0.001$	13.78
October 2008	0.03	38 ± 11	0.49 ± 0.16	0.82 ± 0.10	0.58, $p < 0.001$	17.88	1.14 ± 0.10	0.83, $p < 0.001$	15.39
November 2008	0	30 ± 12	0.69 ± 0.17	0.18 ± 0.15	0.01, $p = 0.35$	9.57	0.60 ± 0.15	0.21, $p < 0.001$	8.92
December 2008	0	16 ± 8	0.44 ± 0.34	0.06 ± 0.14	0.06, $p = 0.02$	3.9	0.35 ± 0.14	0.50, $p < 0.001$	3.63
January 2009	0	4 ± 3	0.28 ± 0.20	0.12 ± 0.07	0.08, $p = 0.01$	2.03	0.24 ± 0.07	0.17, $p < 0.001$	1.98
February 2009	0	3 ± 2	0.39 ± 0.18	−0.68 ± 0.18	0.89, $p < 0.001$	1.59	−1.41 ± 0.18	0.45, $p < 0.001$	2.75
Annual	0.35	28 ± 13	0.65 ± 0.16	0.93 ± 0.01	0.77, $p < 0.001$	42.64	1.14 ± 0.01	0.95, $p < 0.001$	20.62

available energy, r^2 rises above 0.95, and rmse is more than halved. Additionally, the residuals of this relationship skew positive, for instance when available radiation is negligible or negative, LE_{eq} was also negative but actual LE was positive. This bias along with the energy imbalance helps to explain why the monthly total LE is often 10–30% higher than monthly LE_{eq}, yet α_{PT} remains around 1.0. Over the whole measurement period, the two methods generate α_{PT} values of 0.93 and 1.14 (when $R_a = R_n - G - Q_m$ or $R_a = H + LE$, respectively).

3.2. Conductance terms and their drivers

On a monthly basis, mean g_a and g_c were generally of similar magnitude, and both increased during the growing season (Table 4). The uncertainties around these values are substantial when averaging across different time periods within either the diurnal or seasonal cycle, driven as they are by quickly changing synoptic factors. Comparing wet to dry data intervals, defined by the presence rainfall in the preceding 12 h, wetter periods generated higher canopy conductance, with reduced resistance to surface water availability and more direct evaporation. There were negligible differences between wet and dry periods in the aerodynamic conductance. During the growing season 43% of the time was classified as "wet". The mid-summer average canopy conductance during wet periods (16–21.2 mm s^{-1}) exceeded dry-period canopy conductance (10.9–18.1 mm s^{-1}) as well as wet-period aerodynamic conductance (14.1–16.4 mm s^{-1}). The peak monthly mean g_a occured in November (17.0 ± 6.7 mm s^{-1}) and the peak monthly mean g_c occurred in September (28.0 ± 5.7 mm s^{-1}).

Similarly to their monthly average values, the canopy conductance and aerodynamic conductance were of similar magnitude to each other throughout the diurnal cycle (Fig. 4), particularly in the summer months. The drivers of canopy conductance vary substantially during the diurnal course and also within a given month. The time-course of VPD closely followed that of temperature, and both lag incoming radiation (expressed either as PAR or R_g). The conductance terms both tended to reach their maximum between the daily peaks of PAR and VPD (at approximately 14:00, compared to approximately 12:00 or 17:00, respectively). Mean diurnal wind speed (u) peaked around 14:30 in April, peaked earlier in July (12:00) and then peaked around 13:00 for the remainder of the growing season. This timing is consistent with creating an

Table 4
The aerodynamic and canopy resistance terms (g_a and g_c, respectively) are monthly averages of data determined from modeling eddy covariance measurements of water vapor flux. Annual values are derived from the full measurement dataset. Wet values are the mean of time intervals within 12 h of a rain event or on days with snow cover; dry values average other periods.

Month	g_a (mm s^{-1})	g_c (mm s^{-1})	Wet g_c (mm s^{-1})	Dry g_c (mm s^{-1})	Wet g_a (mm s^{-1})	Dry g_a (mm s^{-1})
April 2008	11.2 ± 6.8	12.0 ± 2.3	11.9 ± 2.4	12.4 ± 1.4	10.6 ± 6.5	14.2 ± 7.9
May 2008	14.1 ± 8.2	18.6 ± 5.3	20.7 ± 3.9	17.7 ± 5.7	17.8 ± 6.7	12.5 ± 8.2
June 2008	14.2 ± 7.4	15.7 ± 5.9	18.6 ± 6.2	14.5 ± 5.4	16.4 ± 7.0	13.3 ± 7.5
July 2008	14.2 ± 9.1	12.6 ± 6.8	16.0 ± 6.6	10.9 ± 6.2	14.1 ± 8.5	14.2 ± 9.3
August 2008	15.4 ± 8.5	20.2 ± 4.9	21.2 ± 4.1	18.1 ± 5.6	15.1 ± 8.2	15.9 ± 9.0
September 2008	14.8 ± 8.5	28.0 ± 5.7	28.4 ± 5.8	27.3 ± 5.5	16.0 ± 8.6	13.4 ± 8.0
October 2008	15.7 ± 8.7	10.9 ± 1.0	11.0 ± 1.0	10.8 ± 0.9	17.2 ± 8.1	14.8 ± 8.9
November 2008	17.0 ± 6.7	10.5 ± 0.3	10.5 ± 0.3	10.5 ± 0.3	16.1 ± 6.8	18.0 ± 6.5
December 2008	12.7 ± 5.7	10.5 ± 0.2	10.5 ± 0.2	10.5 ± 0.1	13.2 ± 5.7	11.3 ± 5.7
January 2009	7.9 ± 6.6	10.6 ± 0.6	10.6 ± 0.6	–	7.9 ± 6.6	–
February 2009	7.4 ± 4.7	10.8 ± 0.8	10.8 ± 0.8	–	7.4 ± 4.7	–
Annual	13.5 ± 8.1	14.8 ± 6.8	14.8 ± 6.7	14.8 ± 6.9	13.0 ± 7.9	14.1 ± 8.3

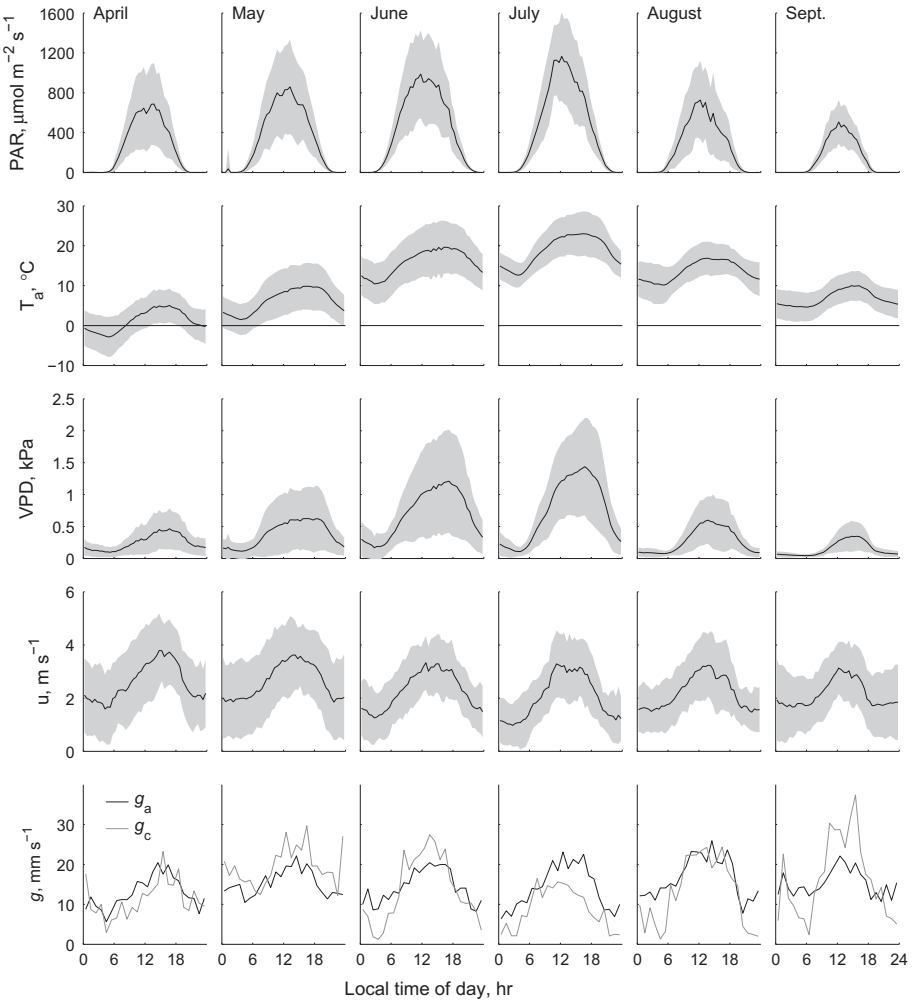

Fig. 4. Diurnal patterns of aerodynamic conductance g_a and canopy conductance g_c and their drivers by month during the growing season; values are the mean of all measurements for each data-collection interval. No gap-filling data were used for the conductance terms. The shading around the driver variables represents one standard deviation. The drivers are presented at half-hourly intervals; the conductance terms are presented at hourly intervals.

aerodynamic conductance value that varied relatively synchronously with canopy conductance. For gap-filling during cases when the sonic anemometer failed, g_a was determined using a derived estimate of u_* from the assumed logarithmic profile of wind speed. The g_a estimates from this model have a root-mean-square error (rmse) of 4.6 mm s^{-1} (r^2 = 0.71, p < 0.001) when compared to periods with valid sonic anemometer estimates of friction velocity.

The wide diurnal peaks of VPD, T_a, and u contributed to similarly broad diurnal peaks in the decoupling coefficient Ω (Fig. 5). This parameter changed little during daytime and only declined in the evening hours when the contribution of R_n to ET was minimal. During the main summer growing season, the mid-day Ω varied little, with monthly mean values in the range 0.65–0.73 (and standard deviation <0.2). The small but inconsistent scatter across

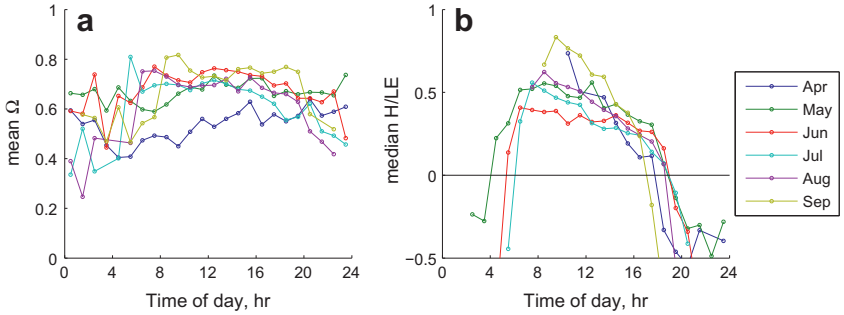

Fig. 5. Monthly mean diurnal evolution of (a) the decoupling factor Ω and (b) the Bowen ratio (H/LE), calculated by binning data into hourly intervals during periods with valid eddy covariance measurements of the sensible heat (H) and latent energy (LE) fluxes. The mid-day standard deviation for Ω is always less than 0.2; the mid-day standard deviation for the Bowen ratio (in May–September) is always less than 0.25.

each month's mean diurnal pattern prevented detecting a clearly defined peak, but most months seemed to have peak Ω at around 12:00 followed by a gentle decline into the late afternoon and evening hours, reflecting the general shift of influence from R_n at mid-day towards VPD later on.

The surface canopy conductance was reduced in response to increasing VPD (Fig. 6 and Table 5). This response appears to be stronger later in the growing season, as indicated by higher values of the c parameter (Table 5) and reduced g_c under similar VPD conditions relative to earlier in the year (Fig. 6). The parameter estimates for the terms in Eq. (8) (Table 5) reveal the uncertainty inherent in this approach, with relatively high error bars (ranging from 10% to 50% of the parameter estimates) and low r^2 (maximum monthly explanatory power in July of 0.35; $p < 0.01$). Day of year explained 24% of the variation in the modeled g_c residuals ($p \sim 0.001$), while water table depth (insignificantly) explained 4% ($p = 0.16$), with higher water tables associated with higher g_c values. The g_c residuals switched from likely positive to likely negative on 9 July, which roughly coincides with maximum vegetation cover (i.e., the completion of the main plant growth period). The relationship between daily mean g_c and VPD (Fig. 6) has relatively high uncertainty bounds on the parameter estimates. The extent of this uncertainty is made clearer by the changes in these parameters given different PAR thresholds. When more data are included by relaxing the PAR threshold, more low-VPD periods are included that have much higher g_c values. This inclusion increases the apparent sensitivity of g_c to VPD by raising b_D, without much demonstrable change in the g_c-VPD relationship at the region of real interest (i.e., high VPD). For half-hourly intervals with VPD >1 kPa, the g_c-VPD slope was -5.7 ± 1.3 mm s^{-1} kPa^{-1} ($r^2 = 0.18$, $p < 0.001$, $n = 316$).

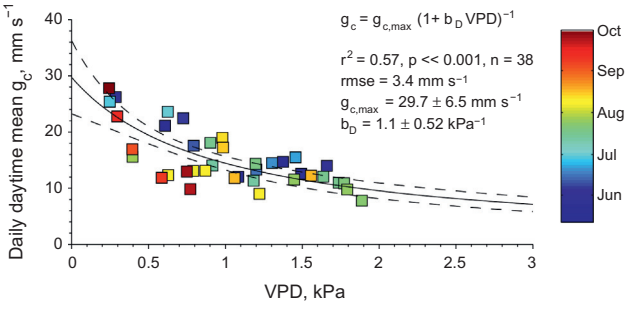

Fig. 6. Daily average canopy conductance g_c plotted against vapor pressure deficit (VPD), where daily values are only calculated when GAI >0.05, there are 6 h or more since last rain, PAR exceeds 400 μmol m^{-2} s^{-1}, and <50% gaps within daytime (10:00–17:00 local time). Points are colored by day of year; the model is fit via nonlinear ordinary least squares regression.

3.3. Evapotranspiration in the water cycle

In addition to its role in the surface energy balance, water vapor fluxes expressed as ET can be related to other terms in the hydrological cycle (Table 6). While the water budget is incomplete due to the lack of in- and outflow measurements, this analysis reveals that ET (406 mm in the period April to October) was roughly in balance with rainfall (389 mm). ET exceeded precipitation during May, June, and July, and was a much less substantial water balance term in the later months. As well as ET exceeding rainfall in these early months, the relatively large drop in the water table indicates additional net outflows of surface or near-surface water in the months through July. This period is followed by net inflow in August and October, with September's lateral water fluxes nearly in balance. The pattern of P – ET generally controlled the behavior of the water table, which declined until its large increase following a rain event in August. During the growing season (DOY 140–260), ET averaged 2.5 mm d^{-1}, with a maximum daily rate of 5.6 mm d^{-1} on 6 July 2008.

4. Discussion

Recent ecological work in this region has described the territory of the Komi Republic as characterized by surplus moisture, i.e., that the annual rainfall significantly exceeds mean annual evapotranspiration (Lopatin et al., 2006). Previous work has also characterized the water balance of bogs in the oligotrophic zones of European Russia and suggested that bogs in the study region fit within 225–250 mm y^{-1} evaporation isolines, with evaporation in "unbogged parts" in the range 275–300 mm y^{-1} (Romanov, 1968b). This study's site had significantly higher annual evapotranspiration (408 mm) than these previous estimates, though during this study year more precipitation was recorded at the Syktyvkar meteorological station than the long-term average. The general lack of high-precision estimates of the latent energy fluxes, and conflicting descriptions of these mires' behavior, allow the current study to suggest some functional overview to the energy balance terms of the fen portion of one of these mires. By many indicators of wetland evapotranspiration, including the Priestley–Taylor α_{PT} term, atmospheric decoupling term Ω, Bowen ratio, and the vertical water balance, the studied fen site in the Ust-Pojeg river valley peatland behaved similarly to open fens in other boreal zones. The site's ample water supply (and high water table) allowed an evapotranspiration flux primarily driven by net radiation.

In its general energy balance characteristics, the Ust-Pojeg fen site is similar to other wetlands. The mid-summer shortwave radiation albedo (monthly mean values from 0.10 in June, peaking at 0.19 in August) and the radiation efficiency ratio (R_n/SW$_{in}$; with mid-summer monthly mean values ranging from 0.45 to 0.61)

Table 5
Monthly fit parameters for g_c model, i.e., eqn. 8 (values from October were used for gap-filling in later months, when low PAR conditions and more frequent measurement errors precluded new parameterizations).

Month	a (mm s^{-1} W^{-1} m^2)	b (mm s^{-1})	c (kPa^{-1})	rmse (mm s^{-1})	r^2
April 2008	0.015 ± 0.012	13.8 ± 3.7	1.37 ± 0.93	9.2	0.11, $p \ll 0.01$ (n = 297)
May 2008	0.052 ± 0.019	21.4 ± 2.8	2.03 ± 0.72	11.2	0.22, $p \ll 0.01$ (n = 554)
June 2008	0.062 ± 0.020	23.7 ± 3.7	2.66 ± 0.84	8.8	0.31, $p \ll 0.01$ (n = 438)
July 2008	0.180 ± 0.103	34.1 ± 10.5	10.28 ± 5.70	7.2	0.35, $p \ll 0.01$ (n = 473)
August 2008	0.049 ± 0.026	27.3 ± 4.2	3.21 ± 1.38	9.4	0.23, $p \ll 0.01$ (n = 400)
September 2008	0.014 ± 0.023	36.9 ± 5.7	3.10 ± 1.29	11.2	0.24, $p \ll 0.01$ (n = 341)
October 2008	0.018 ± 0.036	10.4 ± 5.4	−0.48 ± 1.57	7.9	0.08, p = 0.08 (n = 38)

Table 6
Monthly surface water balance terms including the residual term R (positive residual implies a net inflow; negative residual implies a net outflow). Snowfall was measured at the Syktyvkar weather station approximately 50 km from the field site and is presented in terms of its water equivalent. All terms have units of mm.

Month	Rain	Snow	ET	ΔWT (n = 2)	R (if S_y = 0.6)
April 2008	29.2	8.1	23.8	−32.5 ± 28.5	−14.1
May 2008	48.8	3.3	73.5	−26.4 ± 2.2	−40.5
June 2008	48.6	0	101.1	−58.9 ± 4.4	−87.8
July 2008	49.4	0	105.2	−88.4 ± 19.7	−108.8
August 2008	134.4	0	56.4	141.1 ± 11.0	162.6
September 2008	45.4	0	30.1	−13.9 ± 2.2	7
October 2008	32.8	2.6	9.3	1.5 ± 2.2	24.4
November 2008	0	27.9	4.3	–	−4.3
December 2008	0	15.3	1.1	–	−1.1
January 2009	0	22.4	0.5	–	−0.5
February 2009	0	18.6	0.7	–	−0.7
Sum	388.6	98.2	406.0	−77.5	−63.9

are similar to those found in other boreal wetlands (den Hartog et al., 1994; Lafleur et al., 1997). Even more so than other wetlands surveyed (Lafleur, 2008), the Ust-Pojeg latent energy fluxes are the most significant component of its energy budget (with summer monthly averages greater than 70%). Modeled Q_m is significant in the late spring snowmelt period while it has a similar (and low) magnitude to LE throughout the winter months. On a monthly and daily basis, H is generally of higher magnitude than G. The method to derive G has some error in its assumed heat capacity, which may change over time but is given a static value in the current study. Additionally, the two heat flux plates may not adequately cover the range of microtopographic sites within the fen. Such caveats aside, however, G composes a sizeable portion of the summer energy balance (greater than 10% on a cumulative basis in June, and greater than 15% on selected days' cumulative energy flux). We are therefore hesitant to support the presumption (Peichl et al., 2013) that on the daily time scale G may be neglected as a small contributor to the energy balance. The challenge of measuring available radiation as $R_n - G - Q_m$ has also introduced different methods for determining the Priestley–Taylor factor α_{PT}, which is discussed next.

The α_{PT} at the site explored in this study (0.95–1.05 in the peak growing season assuming R_a is composed of $R_n - G - Q_m$) was similar to other open boreal fens, but higher than other boreal peatland types (both treed fens and open bogs). Determining this value involved some uncertainty deriving from the incomplete energy budget closure, a problem similarly explored elsewhere in relationship to the derived canopy conductance (Wohlfahrt et al., 2009). If α_{PT} was estimated using the sum of H and LE for available energy, rather than ($R_n - G - Q_m$), α_{PT} was 3–65% higher (depending on the month), and had a growing season monthly average always greater than 1.06 (up to 1.34). Previous reviews and studies have used each strategy: some use $R_n - G - Q_m$ (Brümmer et al., 2012; Roulet and Woo, 1986), while others use H + LE (Humphreys et al., 2006; Sonnentag et al., 2010; Souch et al., 1996). The first method is probably better for modeling purposes when the turbulent fluxes are unavailable, but the second is probably better for describing the behavior of the measured LE fluxes given its reduction in the measurement footprint's mismatch. Additional considerations should be made for the corrections necessary for tube-wall adsorption on closed-path sensors (Massman and Ibrom, 2008; Runkle et al., 2012; Nordbo et al., 2013). For two peatlands in Canada (Brümmer et al., 2012), the annual average (daytime, dry-foliage) Priestley–Taylor α_{PT} was in the range 0.55–0.57 (Alberta Western Peatland, a treed, moderately rich fen, 54°57′N, 112°28′W) and 0.74–0.92 (Ontario Eastern Peatland, or Mer Bleue, an ombrotrophic, nutrient-poor bog with more non-vascular ground cover, 45°25′N, 75°31′W). Mid-summer daily peaks of α_{PT} at this latter site may be as high as 1.5 (Admiral et al., 2006). A third Canadian peatland (53°48′N, 104°37′W), the open, moderately rich Sandhill fen site in Saskatchewan, had mean daily mid-day α_{PT} values between 0.99 and 1.04 in three wet years and 0.79 during dry conditions (Sonnentag et al., 2010). A survey of seven Canadian peatlands found mid-summer α_{PT} values in a range from 0.82 to 1.05, used to suggest some physiological limitations to LE flux (Humphreys et al., 2006). In this survey, the two poor fens (a part of Mer Bleue and one near Lac La Biche, Alberta, 55°54′N, 112°33′W) had the highest estimates of α_{PT}, in comparison to the bog part of Mer Bleue, two wooded fens and two extreme-rich fens. Finally, the Swedish carpet-lawn fen Degerö Stormyr had a five-year, growing-season average α_{PT} of 0.98, ranging from 0.86 to 1.17, and derived from ignoring G as relatively insignificant (Peichl et al., 2013).

The relatively high α_{PT} values for the study site imply a stronger control by radiation than vapor pressure deficit in driving evapotranspiration. This characteristic is also implied by the atmospheric decoupling term Ω, which may be higher for open fens than for either treed fens or bog sites. A recent survey of Canadian sites also evaluated their decoupling coefficients, which were 0.16 for three years at the treed fen and in the range 0.29–0.34 for the eastern bog (Brümmer et al., 2012). Our site had higher Ω values in the range around 0.65 in the growing season. This value was relatively insensitive to small changes in formulating g_a or g_c (e.g., which value of kB^{-1} to use). These values are similar to an open fen in Minnesota (Kim and Verma, 1996), but higher than some other open fen sites (Table 7). The values at the study site are also higher than those at the Fyodorovskoye peat bog in Western Russia (56°27′N, 32°55′E), which ranged between 0.2 and 0.5 and were shown to be reduced as the peat surface dried and as vascular plants contributed a proportionately larger amount of measured water vapor fluxes, relative to open-water and moss-dominated surfaces (Kurbatova et al., 2002). They also exceed reported values (0.3–0.5) from three years of eddy covariance measurements at the Zotino bog, a 5 km^2 mixed *Sphagnum*-vascular landscape surrounded by a *P. sylvestris* forest in Western Siberia (60°45′N, 89°23′E) (Kurbatova et al., 2002). Higher values indicating strong decoupling and near complete evaporative control by net radiation

Table 7
Comparative review of energy balance indicators for different boreal fen sites. The Bowen ratio is defined as H/LE, the decoupling coefficient is defined in the text (Eq. (10)), the canopy and aerodynamic conductance terms are given as g_c and g_a, respectively.

Site name	Peatland description	Latitude	Longitude	Location	Bowen ratio	Decoupling coefficient, Ω	Conductance terms, g_c or g_a	Reference
Ust-Pojeg	Fen	61°56′N	50°13′E	Komi, Russia	Summer cumulative value 0.24, but mid-day averages 0.33–0.63	Around 0.65 in the growing season and less (to 0.27) in the winter	g_a and g_c in range 12–26 mm s^{-1} (similar magnitude)	This study
Kaamanen	Open flark fen	69°08′N	27°17′E	N. Lapland, Finland	Mid-day, summer-time, 0.74	n/a	n/a	Aurela et al. (2001)
Degerö Stormyr	Oligotrophic fen	64°11′N	19°33′E	Västerbotten, Sweden	Five-year average, midday growing season as 0.86 ± 0.08	Low (qualitative estimate from g_a/g_s relationship)	g_a 20 mm s^{-1}, g_c 5 mm s^{-1}	Peichl et al. (2013)
Salmisuo	Fen/bog mire	62°46′N	30°58′E	N. Karelia, Finland	Drier year 2006 (Bowen ratio 0.2–0.3) cf. wetter 2007 season (Bowen ratio ~0.5)	n/a	g_c mean was 7.8 mm s^{-1} (range 4–20 mm s^{-1}), g_a not reported	Wu et al. (2010)
Churchill sedge fen	Permafrost sedge fen	58°40′N	94°40′W	Manitoba, Canada	0.48 (average annual); 0.2–0.3 (mid-summer cumulative value)	n/a	g_c (daily mean ~11 mm s^{-1}; noontime values up to 59 mm s^{-1}) g_a daily mean in range from 7–35 mm s^{-1}, noontime values ~ 18 mm s^{-1}	Rouse (2000), Eaton et al. (2001) and Raddatz et al. (2009)
Thompson, Northern Study Area	Rich fen	55°54′N	98°24′W	Manitoba, Canada	Cumulative, 0.46 during green period; daytime values are closer to 1	n/a	n/a	Lafleur et al. (1997)
Near Lac La Biche	Poor fen	55°54′N	112°33′W	Alberta, Canada	Mid-day mid-summer, 0.25–0.4	n/a	$g_{a,noon}$ ~20 mm s^{-1} $g_{c,noon}$ ~12–13 mm s^{-1}	Glenn (2005), Glenn et al. (2006) and Humphreys et al. (2006)
Alberta Western Peatland/Tony's Fen	Treed, moderately rich fen	54°57′N	112°28′W	Alberta, Canada	Approximately 1, lower from late spring values exceeding 2 as the growing season progressed and the sedge canopy density increased	0.16 for three years	$g_{a,noon}$ ~40 mm s^{-1} $g_{c,noon}$~9 mm s^{-1}	Glenn (2005), Glenn et al. (2006), Humphreys et al. (2006) and Brümmer et al. (2012)
Sandhill fen	Fen	53°48′N	104°37′W	Saskatchewan, Canada	n/a	n/a	g_c in range 3.9–4.6 mm s^{-1} (very weak or no response between g_c and VPD), g_a not reported	Sonnentag et al. (2010)
Bog Lake Peatland	Oligotrophic, open *Sphagnum* fen	47°32′N	93°28′W	Minnesota, USA	0.3–0.4 (AM), 0.6–1.0 (PM)	Ranged from 0.55 to 0.89	g_c in range 2–15 mm s^{-1} g_a most often greater than g_c	Kim and Verma (1996)

(Ω > 0.82, approaching 0.99 in the growing season) were found in a freshwater marsh in northeastern China (Sun and Song, 2008).

The higher Ω values at the study site are related to the similar magnitude between g_c and g_a through the year. Many of the other boreal fen sites reviewed in Table 7 show g_c less than g_a, implying a relatively low Ω value. This difference may derive from the study site's relatively high water table (always higher than 20 cm below surface) allowing capillary and root transport from the mire groundwater. This connection is slightly strengthened when considering the month of July at the site, when g_c reaches its mid-summer low. Unfortunately the synchronicity of the relatively low water table and highest VPD rates preclude a clear interpretation of the drivers of this low g_c, though the statistical look at residuals of Eq. (9) suggests a larger role for VPD than the water table. Phenological factors may also play a role in this reduced g_c, as the reduction starts following the peak in vegetation cover. Three of the Canadian peatlands surveyed by Humphreys et al. (2006), two wooded fens and a rich fen, showed a stronger (b_D > 1 kPa^{-1}) response of canopy conductance to VPD, though the other sites had a weaker relationship (b_D < 0.3 kPa^{-1}) than this study's data indicate (b_D < 1.1 ± 0.52 kPa^{-1}). The Glencar Atlantic blanket bog in Ireland (51°55′N, 9°55′W) had a stronger response (b_D = 8.6 kPa^{-1}) though as in the current study, the relationship had a relatively weak fit (r^2 < 0.40) and indicates more of a qualitative than exact control by VPD (Sottocornola and Kiely, 2010). A recent study of errors in ET models finds higher predictive uncertainty in landscapes with low Ω or high controls by surface conductance on ET (Polhamus et al., 2013). This finding implies that it may be easier to make ET predictions of these landscapes using well-defined radiation terms rather than more difficult biophysical parameterizations of the transpiring surface vegetation. The implication for modeling studies on these boreal fen landscapes is that they require less detail on the surface scale and interactions between VPD, g_c, surface wetness, and ET.

The site's Bowen ratio (a summer average via total cumulative fluxes of 0.24, but mid-day averages in the range 0.33–0.63) was relatively low compared to other peatland field sites. In particular, two relatively nearby northern European fens (Aurela et al., 2001; Peichl et al., 2013), which may otherwise be considered as analogous to the study site, showed higher average mid-day summertime Bowen ratios (Table 7). The Bowen ratios of two other poor fens (Kim and Verma, 1996; Glenn et al., 2006) and a Finnish fen/bog mire (Wu et al., 2010) are more comparable to the study site. The study site's Bowen ratios may also be comparable to low values found at some Russian peatland bogs: for the two Russian bogs mentioned previously (Kurbatova et al., 2002) mid-summer values of approximately 0.3 (Zotino) and 0.4–0.8 (Fyodorovskoye) were reported. At another West Siberian continental bog (56°51′N, 82°50′E), the summer Bowen ratio ranged from 0.57 during the early growing season and up to 0.78 in the peak growing season (Shimoyama et al., 2003), so the similarities to Russian bogs may not be universal. Similarly, the Stormossen bog in central Sweden (60°07′N, 17°05′E) had a reported mid-summer minimum Bowen ratio of 0.6 (Kellner, 2001). A recent review of wetland evaporation found higher summer median (cumulative flux) values in both fens (0.46) and bogs (0.6) and roughly similar values for marshes (0.25), though with a fairly small number of studies in each group (n from 5 to 7) (Lafleur, 2008). In the study site, at least, the comparatively low Bowen ratio appears to be driven by the relatively high water table and the associated high surface conductance values.

The study site's mean daily growing season ET rate (2.5 mm d^{-1}; peak 5.8 mm d^{-1}) is comparable to some of the wetland sites in its latitude band, as reviewed by Lafleur (2008, Fig. 10). In particular, these evapotranspiration rates are similar in magnitude to the Danish riparian wetland (56°22′N, 9°41′E) studied by Andersen et al. (2005), who found average ET rates of 3.6 mm d^{-1} (peak of 5.6 mm d^{-1}), accounting for 82% of daytime net radiation. These evaporation rates are also similar to those found in the Bog Lake Peatland of Minnesota (47°32′N, 93°28′W), an oligotrophic, open *Sphagnum* fen with growing season average 3.0 mm d^{-1} (peak 4.8 mm d^{-1}) and with fen ET 85–115% of potential ET (Kim and Verma, 1996). Similarly, a *Carex lasiocarpa* marsh in China's Sanjiang Plain (47°35′N, 133°31′E) showed daily ET rates averaging 2.3 mm d^{-1} (peak 4.8 mm d^{-1}) and α_{PT} of 1.01 (using $R_n - G$ for R_a) (Sun and Song, 2008; Guo and Sun, 2011). The previously mentioned Finnish site, Salmisuo, had comparable growing season daily ET rates of 2.23 mm d^{-1} and 1.59 mm d^{-1} for its dry and wet years, respectively, with a peak rate of 5.0 mm d^{-1} (Wu et al., 2010).

Finally, the study site's roughness length changed with season more than stability or wind direction, and so was presented as a monthly mean (Table 3). The roughness length estimate (peaking at 46 ± 12 mm) is comparable to a Quebec natural bog with *Sphagnum* hummocks and low ericaceous (i.e., acid-loving) shrubs, where z_0 was modeled from wind profile data as 40.9 mm (Campbell et al., 2002). Average z_0 estimates of 18.6 mm (ranging from 10 to 30 mm) have been determined for a Swedish bog named Ryggmosen (Mölder and Kellner, 2002). During the snow-free period in Canada's Mer Bleue bog, a constant z_0 value of 77 ± 1 mm was derived from sonic anemometer data (Lafleur et al., 2005). Other estimates of z_0 for peatlands are in the range 20–70 mm for a Siberian bog (Shimoyama et al., 2004), or 21–32 mm for a Swedish mire nearby Ryggmosen (Kellner, 2001). The northern Finnish flark fen Kaamanen had z_0 of 80 mm (Aurela et al., 2001), and the Swedish carpet-lawn fen Degerö Stormyr had z_0 up to 30 mm (Peichl et al., 2013). This range of values is indicative of the variety of peatland types and vegetation cover, and places the Ust-Pojeg site studied here, with its low vegetation and slight hummock features, in the mid-range of the peatlands surveyed.

5. Conclusions

We have generated an 11-month energy balance for the oligotrophic fen portion of a mixed bog-fen river valley peatland in the boreal zone of European Russia by supplementing eddy covariance measurements with gap-filling models and in situ measurements of non-turbulent energy fluxes and associated meteorological terms. The evapotranspiration flux may reasonably be estimated using the Priestley–Taylor method, provided adequate assumptions about the energy balance closure can be provided. The growing season energy balance (April–September) was dominated by evapotranspiration, which seemed largely governed by net radiation at the surface with a lower-level control provided by vapor pressure deficit in its role in restricting the canopy conductance. The canopy conductance was higher earlier in the growing season than later in the season, with the reduction starting roughly coincident with the peak vegetation cover. Canopy conductance was higher than at other similar sites in the boreal zone, perhaps due to the relatively high water table. During the period April–October 2008, evapotranspiration (399.4 mm) nearly balanced rainfall (402.6 mm). High snowfall (84.2 mm water equivalent) and limited evapotranspiration (6.6 mm) during the rest of the year generated an annual atmospheric water budget with excess incoming water. On a monthly basis, the growing season months of May–July had nearly twice the evapotranspiration as precipitation. Disentangling the roles of vascular plant cover and water table height in controlling the energy balance, and particularly the latent energy flux term, is challenging to do for the dataset in this study and should be encouraged as a target of future studies. However, the higher decoupling coefficient and predominance of

R_n in driving ET lend encouragement to relatively simplistic modeling approaches for this landscape.

Acknowledgements

B. Runkle, C. Wille, and L. Kutzbach are supported by the Cluster of Excellence "CliSAP" (EXC177; Integrated Research Activity 08/2-034) of the University of Hamburg, as funded by the German Research Foundation (DFG). Support for open-access publishing was provided through a fellowship to B. Runkle from the University of Hamburg's Center for a Sustainable University (KNU). Field work was conducted by the Emmy Noether Independent Research Group led by M. Wilmking and funded by the German Research Foundation (Wi 2680/2-1). Infrastructure and field work was partially supported by the CARBO-North Project (6th FP of the EU, Contract number 36993). In addition, we thank and acknowledge Svetlana Zagirova and other members of the Komi Science Centre for their logistical support. We appreciate the field data collection and logistical support of Peter Schreiber, Julia Schneider, and Oleg Mikhaylov, and the footprint modeling by Inke Forbrich. We appreciate suggestions from Armine Avagyan that helped improve the manuscript and assistance in mapping from Sebastian Zubrzycki. We thank the two anonymous reviewers for their useful suggestions.

Appendix A. Supplementary material

Supplementary data associated with this article can be found, in the online version, at http://dx.doi.org/10.1016/j.jhydrol.2014.01.056.

References

Admiral, S.W., Lafleur, P.M., Roulet, N.T., 2006. Controls on latent heat flux and energy partitioning at a peat bog in eastern Canada. Agric. Forest Meteorol. 140, 308–321.

Andersen, H.E., Hansen, S., Jensen, H.E., 2005. Evapotranspiration from a riparian fen wetland. Nordic Hydrol. 36, 121–135.

Apps, M.J., Kurz, W.A., Luxmoore, R.J., Nilsson, L.O., Sedjo, R.A., Schmidt, R., Simpson, L.G., Vinson, T.S., 1993. Boreal forests and tundra. Water Air Soil Pollut. 70, 39–53.

Aurela, M., Laurila, T., Tuovinen, J.-P., 2001. Seasonal CO_2 balances of a subarctic mire. J. Geophys. Res.: Atmos. (1984–2012) 106, 1623–1637.

Baldocchi, D.D., 2003. Assessing the eddy covariance technique for evaluating carbon dioxide exchange rates of ecosystems: past, present and future. Global Change Biol. 9, 479–492.

Batjes, N.H., 1996. Total carbon and nitrogen in the soils of the world. Eur. J. Soil Sci. 47, 151–163.

Billett, M.F., Palmer, S.M., Hope, D., Deacon, C., Storeton-West, R., Hargreaves, K.J., Flechard, C., Fowler, D., 2004. Linking land-atmosphere-stream carbon fluxes in a lowland peatland system. Global Biogeochem. Cycles 18.

Bolton, D., 1980. The computation of equivalent potential temperature. Monthly Weather Rev. 108, 1046–1053.

Bridgham, S.D., Pastor, J., Dewey, B., Weltzin, J.F., Updegraff, K., 2008. Rapid carbon response of peatlands to climate change. Ecology 89, 3041–3048.

Brümmer, C., Black, T.A., Jassal, R.S., Grant, N.J., Spittlehouse, D.L., Chen, B., Nesic, Z., Amiro, B.D., Arain, M.A., Barr, A.G., Bourque, C.P.-A., Coursolle, C., Dunn, A.L., Flanagan, L.B., Humphreys, E.R., Lafleur, P.M., Margolis, H.A., McCaughey, J.H., Wofsy, S.C., 2012. How climate and vegetation type influence evapotranspiration and water use efficiency in Canadian forest, peatland and grassland ecosystems. Agric. Forest Meteorol. 153, 14–30.

Brutsaert, W., 1982. Evaporation into the Atmosphere: Theory, History, and Applications. Reidel, Dordrecht.

Campbell, D.I., Williamson, J.L., 1997. Evaporation from a raised peat bog. J. Hydrol. 193, 142–160.

Campbell, D.R., Lavoie, C., Rochefort, L., 2002. Wind erosion and surface stability in abandoned milled peatlands. Can. J. Soil Sci. 82, 85–95.

Comer, N.T., Lafleur, P.M., Roulet, N.T., Letts, M.G., Skarupa, M., Verseghy, D., 2000. A test of the Canadian land surface scheme (CLASS) for a variety of wetland types. Atmosphere-Ocean 38, 161–179.

Couwenberg, J., Joosten, H., 2005. Self-organization in raised bog patterning: the origin of microtope zonation and mesotope diversity. J. Ecol. 93, 1238–1248.

Den Hartog, G., Neumann, H.H., King, K.M., Chipanshi, A.C., 1994. Energy budget measurements using eddy correlation and Bowen ratio techniques at the Kinosheo Lake tower site during the Northern Wetlands Study. J. Geophys. Res. 99, 1539–1549.

Dise, N.B., 2009. Peatland response to global change. Science 326, 810–811.

Drexler, J.Z., Snyder, R.L., Spano, D., Paw U, K.T., 2004. A review of models and micrometeorological methods used to estimate wetland evapotranspiration. Hydrol. Process. 18, 2071–2101.

Eaton, A.K., Rouse, W.R., Lafleur, P.M., Marsh, P., Blanken, P.D., 2001. Surface energy balance of the western and central Canadian subarctic: variations in the energy balance among five major terrain types. J. Climate 14, 3692–3703.

Eichinger, W.E., Parlange, M.B., Stricker, H., 1996. On the concept of equilibrium evaporation and the value of the Priestley–Taylor coefficient. Water Resour. Res. 32, 161–164.

ESA, 2010. GlobCover 2009 (Global Land Cover Map) Released on 21 December; <http://due.esrin.esa.int/globcover/>.

Falge, E., Baldocchi, D., Olson, R., Anthoni, P., Aubinet, M., Bernhofer, C., Burba, G., Ceulemans, R., Clement, R., Dolman, H., Granier, A., Gross, P., Grünwald, T., Hollinger, D., Jensen, N.-O., Katul, G., Keronen, P., Kowalski, A., Ta Lai, C., Law, B.E., Meyers, T., Moncrieff, J., Moors, E., William Munger, J., Pilegaard, K., Rannik, Ü., Rebmann, C., Suyker, A., Tenhunen, J., Tu, K., Verma, S., Vesala, T., Wilson, K., Wofsy, S., 2001. Gap filling strategies for long term energy flux data sets. Agric. Forest Meteorol. 107, 71–77.

Foken, T., 2008. Micrometeorology. Springer-Verlag, Berlin Heidelberg.

Foken, T., Wichura, B., 1996. Tools for quality assessment of surface-based flux measurements. Agric. Forest Meteorol. 78, 83–105.

Forbrich, I., Kutzbach, L., Wille, C., Becker, T., Wu, J., Wilmking, M., 2011. Cross-evaluation of measurements of peatland methane emissions on microform and ecosystem scales using high-resolution landcover classification and source weight modelling. Agric. Forest Meteorol. 151, 864–874.

Frolking, S., Talbot, J., Jones, M.C., Treat, C.C., Kauffman, J.B., Tuittila, E.S., Roulet, N., 2011. Peatlands in the Earth's 21st century climate system. Environ. Rev. 19, 371–396.

Gažovič, M., Kutzbach, L., Schreiber, P., Wille, C., Wilmking, M., 2010. Diurnal dynamics of CH_4 from a boreal peatland during snowmelt. Tellus B 62, 133–139.

Gažovič, M., Kutzbach, L., Forbrich, I., Schneider, J., Wille, C., Wilmking, M., in preparation. Temperature and plant phenology control the seasonal variability of CO_2 and CH_4 fluxes from a boreal peatland in North-West Russia.

Glenn, A.J., 2005. Growing Season Carbon Dioxide Exchange of Two Contrasting Peatland Ecosystems. University of Lethbridge, Faculty of Arts and Science, Lethbridge, Alta.

Glenn, A.J., Flanagan, L.B., Syed, K.H., Carlson, P.J., 2006. Comparison of net ecosystem CO_2 exchange in two peatlands in western Canada with contrasting dominant vegetation, *Sphagnum* and *Carex*. Agric. Forest Meteorol. 140, 115–135.

Guo, Y., Sun, L., 2011. Surface energy fluxes and control of evapotranspiration from a *Carex lasiocarpa* mire in the Sanjiang Plain, Northeast China. Int. J. Biometeorol., 1–12.

Humphreys, E.R., Lafleur, P.M., Flanagan, L.B., Hedstrom, N., Syed, K.H., Glenn, A.J., Granger, R., 2006. Summer carbon dioxide and water vapor fluxes across a range of northern peatlands. J. Geophys. Res. 111, 16.

Ivanov, K.E., 1981. Water Movement in Mirelands (Vodoobmen v bolotnykh landshaftakh). Academic Press, London.

Jarvis, P.G., McNaughton, K.G., 1986. Stomatal control of transpiration: scaling up from leaf to region. Adv. Ecol. Res 15, 1–49.

Jobbágy, E.G., Jackson, R.B., 2000. The vertical distribution of soil organic carbon and its relation to climate and vegetation. Ecol. Appl. 10, 423–436.

Joosten, H., Tapio-Biström, M.-L., Tol, S., 2012. Peatlands-guidance for climate change mitigation through conservation, rehabilitation and sustainable use. FAO.

Kellner, E., 2001. Surface energy fluxes and control of evapotranspiration from a Swedish *Sphagnum* mire. Agric. Forest Meteorol. 110, 101–123.

Kim, J., Verma, S.B., 1996. Surface exchange of water vapour between an open *sphagnum* fen and the atmosphere. Boundary-Layer Meteorol. 79, 243–264.

Kormann, R., Meixner, F.X., 2001. An analytical footprint model for non-neutral stratification. Boundary-Layer Meteorol. 99, 207–224.

Kurbatova, J., Arneth, A., Vygodskaya, N.N., Kolle, O., Varlargin, A.V., Milyukova, I.M., Tchebakova, N.M., Schulze, E.D., Lloyd, J., 2002. Comparative ecosystem-atmosphere exchange of energy and mass in a European Russian and a central Siberian bog I. Interseasonal and interannual variability of energy and latent heat fluxes during the snowfree period. Tellus B 54, 497–513.

Lafleur, P.M., 2008. Connecting atmosphere and wetland: energy and water vapour exchange. Geography Compass 2, 1027–1057.

Lafleur, P.M., McCaughey, J.H., Joiner, D.W., Bartlett, P.A., Jelinski, D.E., 1997. Seasonal trends in energy, water, and carbon dioxide fluxes at a northern boreal wetland. J. Geophys. Res. 102, 29009–29020.

Lafleur, P.M., Hember, R.A., Admiral, S.W., Roulet, N.T., 2005. Annual and seasonal variability in evapotranspiration and water table at a shrub-covered bog in southern Ontario, Canada. Hydrol. Process. 19, 3533–3550.

Limpens, J., Berendse, F., Blodau, C., Canadell, J.G., Freeman, C., Holden, J., Roulet, N., Rydin, H., Schaepman-Strub, G., 2008. Peatlands and the carbon cycle: from local processes to global implications – a synthesis. Biogeosciences 5, 1475–1491.

Lopatin, E., Kolstrom, T., Spiecker, H., 2006. Determination of forest growth trends in Komi Republic (northwestern Russia): combination of tree-ring analysis and remote sensing data. Boreal Environ. Res. 11, 341–353.

Lopatin, E., Kolstroem, T., Spiecker, H., Baeck, J., 2008. Long-term trends in radial growth of Siberian spruce and Scots pine in Komi Republic (northwestern Russia). Boreal Environ. Res. 13, 539–552.

Masing, V., Botch, M., Läänelaid, A., 2010. Mires of the former Soviet Union. Wetlands Ecol. Manage. 18, 397–433.

Massman, W.J., Ibrom, A., 2008. Attenuation of concentration fluctuations of water vapor and other trace gases in turbulent tube flow. Atmos. Chem. Phys. 8, 6245–6259.
McNaughton, K.G., 1976. Evaporation and advection I: evaporation from extensive homogeneous surfaces. Quart. J. Roy. Meteorol. Soc. 102, 181–191.
McNaughton, K.G., Jarvis, P.G., 1983. Predicting effects of vegetation changes on transpiration and evaporation. Water Deficits Plant Growth 7, 1–47.
Minayeva, T.Y., Sirin, A.A., 2012. Peatland biodiversity and climate change. Biol. Bull. Rev. 2, 164–175.
Mölder, M., Kellner, E., 2002. Excess resistance of bog surfaces in central Sweden. Agric. Forest Meteorol. 112, 23–30.
Nordbo, A., Kekäläinen, P., Siivola, E., Lehto, R., Vesala, T., Timonen, J., 2013. Tube transport of water vapor with condensation and desorption. Appl. Phys. Lett. 102, 194101-1–194101-5.
Owen, P.R., Thomson, W.R., 1963. Heat transfer across rough surfaces. J. Fluid Mech. 15, 321–334.
Peichl, M., Sagerfors, J., Lindroth, A., Buffam, I., Grelle, A., Klemedtsson, L., Laudon, H., Nilsson, M.B., 2013. Energy exchange and water budget partitioning in a boreal minerogenic mire. J. Geophys. Res.: Biogeosci. 118, 1–13.
Petrone, R.M., Devito, K.J., Silins, U., Mendoza, C., Brown, S.C., Kaufman, S.C., Price, J.S., 2008. Transient peat properties in two pond-peatland complexes in the sub-humid Western Boreal Plain, Canada. Mires Peat 3, 1–13.
Pluchon, N., 2009. The impact of recent paludification rates on the carbon budget of taiga regions—case studies from two peatlands in European Russia (Masters Thesis). Department of Physical Geography and Quaternary Geology, Stockholm University.
Polhamus, A., Fisher, J.B., Tu, K.P., 2013. What controls the error structure in evapotranspiration models? Agric. Forest Meteorol. 169, 12–24.
Priestley, C.H.B., Taylor, R.J., 1972. On the assessment of surface heat flux and evaporation using large-scale parameters. Monthly Weather Rev. 100, 81–92.
Raddatz, R.L., Papakyriakou, T.N., Swystun, K.A., Tenuta, M., 2009. Evapotranspiration from a wetland tundra sedge fen: surface resistance of peat for land-surface schemes. Agric. Forest Meteorol. 149, 851–861.
Rango, A., Martinec, J., 1995. Revisiting the degree-day method for snowmelt computations1. JAWRA J. Am. Water Resour. Assoc. 31, 657–669.
Reichstein, M., Falge, E., Baldocchi, D., Papale, D., Aubinet, M., Berbigier, P., Bernhofer, C., Buchmann, N., Gilmanov, T., Granier, A., Grunwald, T., Havrankova, K., Ilvesniemi, H., Janous, D., Knohl, A., Laurila, T., Lohila, A., Loustau, D., Matteucci, G., Meyers, T., Miglietta, F., Ourcival, J.-M., Pumpanen, J., Rambal, S., Rotenberg, E., Sanz, M., Tenhunen, J., Seufert, G., Vaccari, F., Vesala, T., Yakir, D., Valentini, R., 2005. On the separation of net ecosystem exchange into assimilation and ecosystem respiration: review and improved algorithm. Global Change Biol. 11, 1424–1439.
RIHMI-WDC, 2013. Hydrometeorological data, Baseline Climatological Data Sets, Syktyvkar Site # 23804, <http://meteo.ru/english/data/>.
Romanov, V.V., 1968a. Evaporation from Bogs in the European Territory of the USSR. Israel Program for Scientific Translation, Jerusalem.
Romanov, V.V., 1968b. Hydrophysics of Bogs (Gidrofizika bolot). Israel Program for Scientific Translation.
Roulet, N.T., Woo, M., 1986. Wetland and lake evaporation in the low Arctic. Arctic Alpine Res. 18, 195–200.
Rouse, W.R., 2000. The energy and water balance of high-latitude wetlands: controls and extrapolation. Global Change Biol. 6, 59–68.
Runkle, B.R.K., Wille, C., Gažovič, M., Kutzbach, L., 2012. Attenuation correction procedures for water vapour fluxes from closed-path eddy-covariance systems. Boundary-Layer Meteorol. 142, 401–423.
Schneider, J., Kutzbach, L., Wilmking, M., 2012. Carbon dioxide exchange fluxes of a boreal peatland over a complete growing season, Komi Republic, NW Russia. Biogeochemistry 111, 485–513.
Shimoyama, K., Hiyama, T., Fukushima, Y., Inoue, G., 2003. Seasonal and interannual variation in water vapor and heat fluxes in a West Siberian continental bog. J. Geophys. Res. 108, 4648. http://dx.doi.org/10.1029/2003JD003485, D20.
Shimoyama, K., Hiyama, T., Fukushima, Y., Inoue, G., 2004. Controls on evapotranspiration in a west Siberian bog. J. Geophys. Res. 109, D08111. http://dx.doi.org/10.1029/2003JD004114.
Shutov, V., 2004. Extensive studies in boreal wetland watersheds in northwestern Russia. (Proceedings of a workshop held at Victoria, Canada, March 2004). IAHS Publ. 290, 103–110.
Sonnentag, O., van der Kamp, G., Barr, A.G., Chen, J.M., 2010. On the relationship between water table depth and water vapor and carbon dioxide fluxes in a minerotrophic fen. Global Change Biol. 16, 1762–1776.
Sonnentag, O., Detto, M., Runkle, B.R.K., Teh, Y.A., Silver, W.L., Kelly, M., Baldocchi, D.D., 2011. Carbon dioxide exchange of a pepperweed (*Lepidium latifolium* L.) infestation: how do flowering and mowing affect canopy photosynthesis and autotrophic respiration? J. Geophys. Res. 116, G01021. http://dx.doi.org/10.1029/2010JG001522.
Sottocornola, M., Kiely, G., 2010. Energy fluxes and evaporation mechanisms in an Atlantic blanket bog in southwestern Ireland. Water Resour. Res. 46, W11524. http://dx.doi.org/10.1029/2010WR009078.
Souch, C., Wolfe, C.P., Grimmtind, C.S.B., 1996. Wetland evaporation and energy partitioning: Indiana Dunes National Lakeshore. J. Hydrol. 184, 189–208.
Sun, L., Song, C., 2008. Evapotranspiration from a freshwater marsh in the Sanjiang Plain, Northeast China. J. Hydrol. 352, 202–210.
Vasander, H., 2007. Peatlands. In: Pearson, M., Ojanen, P., Havimo, M., Kuuluvainen, T., Vasander, H. (Eds.), On the European Edge: Journey through Komi Nature and Culture. University of Helsinki, Department of Forest Ecology Publications, University of Helsinki, Department of Forest Ecology, Helsinki, pp. 103–112.
Verma, S.B., 1989. Aerodynamic resistances to transfers of heat, mass and momentum. In: Black, T.A. (Ed.), Estimation of Areal Evapotranspiration. Int. Assoc. Hydrol. Sci, Vancouver, B.C., pp. 13–20.
Wang, K., Dickinson, R.E., 2012. A review of global terrestrial evapotranspiration: observation, modeling, climatology, and climatic variability. Rev. Geophys. 50, RG2005, http://dx.doi.org/10.1029/2011RG000373.
Wesely, M.L., Hicks, B.B., 1977. Some factors that affect the deposition rates of sulfur dioxide and similar gases on vegetation. J. Air Pollution Control Assoc. 27, 1110–1116.
Wilson, K.B., Baldocchi, D.D., 2000. Seasonal and interannual variability of energy fluxes over a broadleaved temperate deciduous forest in North America. Agric. Forest Meteorol. 100, 1–18.
Wohlfahrt, G., Haslwanter, A., Hörtnagl, L., Jasoni, R.L., Fenstermaker, L.F., Arnone III, J.A., Hammerle, A., 2009. On the consequences of the energy imbalance for calculating surface conductance to water vapour. Agric. Forest Meteorol. 149, 1556–1559.
Wu, J., Kutzbach, L., Jager, D., Wille, C., Wilmking, M., 2010. Evapotranspiration dynamics in a boreal peatland and its impact on the water and energy balance. J. Geophys. Res. 115, G04038. http://dx.doi.org/10.1029/2009JG001075.
Yu, Z.C., 2012. Northern peatland carbon stocks and dynamics: a review. Biogeosciences 9, 4071–4085.